Published in final edited form as:

J Immunol. 2019 October 01; 203(7): 1867–1881. doi:10.4049/jimmunol.1900654.

LSD1 cooperates with non-canonical NF-κB signaling to regulate marginal zone B cell development

Robert R. Haines, **Christopher D. Scharer**, **Jenna L. Lobby**, **Jeremy M. Boss**[2]

Department of Microbiology & Immunology, 1510 Clifton Rd, Emory University School of Medicine, Atlanta, GA, USA. 30322

Abstract

Marginal zone B cells (MZB) are a mature B cell subset that rapidly respond to blood-borne pathogens. Although the transcriptional changes that occur throughout MZB development are known, the corresponding epigenetic changes and epigenetic modifying proteins that facilitate these changes are poorly understood. The histone demethylase LSD1 is an epigenetic modifier that promotes plasmablast formation, but its role in B cell development has not been explored. Here, a role for LSD1 in the development of B cell subsets was explored. B cell-conditional deletion of LSD1 in mice resulted in a decrease in MZB while follicular B cells (FoB) and bone marrow B cell populations were minimally affected. LSD1 repressed genes in MZB that were normally upregulated in the myeloid and FoB lineages. Correspondingly, LSD1 regulated chromatin accessibility at the motifs of transcription factors known to regulate splenic B cell development, including NF-κB motifs. The importance of NF-κB signaling was examined through an *ex vivo* MZB development assay, which showed that both LSD1-deficient and NF-κB-inhibited transitional B cells failed to undergo full MZB development. Gene expression and chromatin accessibility analyses of *in vivo*- and *ex vivo*-generated LSD1-deficient MZB indicated that LSD1 regulated the downstream target genes of non-canonical NF-κB signaling. Additionally LSD1 was found to interact with the non-canonical NF-κB transcription factor p52. Together, these data reveal that the epigenetic modulation of the non-canonical NF-κB signaling pathway by LSD1 is an essential process during the development of MZB.

Introduction

B cell progenitors develop through multiple stages to become mature naïve B cells capable of generating a humoral immune response. In the bone marrow, common lymphoid progenitors progress through the pro-B and pre-B cell stages, during which the B cell receptor (BCR) is rearranged to generate a functional yet diverse repertoire of B cells (1). BCR-expressing immature B cells migrate to the spleen where they undergo transitional B cell development, resulting in the formation of follicular B cells (FoB) and marginal zone B cells (MZB). FoB circulate throughout the periphery and facilitate humoral immune responses to antigen and give rise to memory B cells and long-lived plasma cells (1). MZB localize to the splenic marginal sinus and rapidly respond to blood-borne pathogens, primarily forming short-lived plasmablasts (1, 2).

[2]Address correspondence to Jeremy M. Boss, telephone 404-727-5973, jmboss@emory.edu.

Specific signaling mechanisms drive the MZB or FoB cell fate decision. When immature B cells enter the periphery, they undergo positive selection through tonic BCR signaling to promote survival (3). The strength of tonic BCR signaling influences immature B cell fate with stronger signals promoting FoB commitment and weaker signals promoting MZB commitment (3). Immature B cells must experience two additional signaling pathways to further commit to the MZB fate. The first is Notch2 signaling through interaction with the Notch ligand DLL1, which is expressed by splenic venules in the red pulp and marginal zone (1). The second is BAFFR-dependent activation of non-canonical NF-κB signaling (1). Both pathways are necessary for MZB cell development and function in a synergistic manner (1).

Throughout cell fate commitment, MZB acquire a transcriptional identity distinct from FoB that confers specific functional capabilities (1, 2). For example, MZB express high levels of *S1pr1* to facilitate homing to the marginal zone (4) and downregulate the FoB genes *Itgb7*, *Cxcr4*, and *Ccr7* that facilitate homing to secondary lymphoid organs (5). *Myc* is highly expressed in MZB, providing an enhanced capacity to proliferate in response to antigens such as bacterial lipopolysaccharide (LPS) (6). MZB can rapidly respond to other TLR agonists (7) and display a concomitant increase in innate immune sensor molecules relative to FoB, including TLR3, TLR7, TLR9, NOD1/2/3, and NLRC4 (8). Although the MZB transcriptome is characterized, the epigenetic modifications acquired during B cell development that establish it are not well studied. Additionally, the enzymes that facilitate splenic B cell epigenetic remodeling are not known.

Lysine-specific demethylase 1 (LSD1) is a histone demethylase that targets H3K4me1, H3K4me2, H3K9me1, and H3K9me2 through FAD-dependent amine oxidation (9). LSD1-based modification of chromatin results in the fine-tuning of target gene expression, which is critical for driving cellular development (9). Regarding B cell differentiation, LSD1 promotes plasmablast formation and decommissions active enhancers at Blimp-1, PU-1, and IRF4 binding sites through H3K4me1 demethylation and repression of chromatin accessibility (10). LSD1 also promotes germinal center formation by repressing plasma cell genes, such as *Prdm1* and *Irf4*, through enhancer decommissioning facilitated by interaction with BCL6 (11). Despite evidence highlighting a critical role for LSD1 in the epigenetic regulation of B cell differentiation, its *in vivo* role during B cell development has not been explored.

In this study, mice with B-cell conditional deletion of LSD1 were used to examine its function throughout B cell development. Phenotyping revealed that LSD1 was dispensible for the development of bone marrow B cell subsets and FoB but was required for MZB formation. RNA-seq analysis of LSD1-deficient MZB and FoB showed that LSD1 functions as a transcriptional repressor in MZB. Assay for transposase accessible chromatin sequencing (ATAC-seq) analysis revealed a chromatin modulatory role for LSD1 at motifs of transcription factors critical for MZB development, including NF-κB. Experiments using an *ex vivo* MZB development system indicated pathway overlap between LSD1 and non-canonical NF-κB signaling. LSD1 and NF-κB p52 also interact following non-canonical NF-κB stimulation. Overall, these data identify LSD1 as a key transcriptional and epigenetic modifier during MZB development.

Materials and Methods

Data Availability

Sequencing data are available through accession GSE132227 at the NCBI Gene Expression Omnibus (https://www.ncbi.nlm.nih.gov/geo/query/acc.cgi?acc=GSE132227).

Mice and Animal Procedures

LSD1 floxed mice (*Kdm1a*$^{fl/fl}$; 023969; The Jackson Laboratory) (12) were a gift from Dr. David Katz (Emory University). *Kdm1a*$^{fl/fl}$*Cd19*$^{Cre/+}$ mice (referred to as CKO) were created from crossing *Kdm1a*$^{fl/fl}$ mice to *Cd19*$^{Cre/+}$ mice (006785; The Jackson Laboratory) (13). *Kdm1a*$^{+/+}$*Cd19*$^{Cre/+}$ mice (referred to as CreWT) were used as wild-type controls due to the hemizygous nature of the *Cd19* allele (14). *Kdm1a*$^{fl/fl}$*Rosa26*$^{CreERT2/+}$ mice were created from crossing *Rosa26*$^{CreERT2/+}$ mice (008463; The Jackson Laboratory) (15) with *Kdm1a*$^{fl/fl}$ mice. C57BL/6 wild-type mice were obtained from The Jackson Laboratory (000664) and were bred on site. Experiments were performed on mice 8–12 weeks old.

For mixed bone marrow chimera experiments, 1–2 × 10^7 bone marrow cells from *Kdm1a*$^{fl/fl}$*Cd19*$^{Cre/+}$ CD45.1 mice and *Kdm1a*$^{+/+}$*Cd19*$^{Cre/+}$ CD45.1/.2 mice were mixed in a 1:1 ratio and injected into host CD45.2 B6 wild-type mice (000664; The Jackson Laboratory) that were lethally irradiated with 900 rad (two doses of 450 rad six hours apart). Host mice were given water containing 2% sucrose, 10 μg/ml Neomycin (N5285; Sigma-Aldrich), and 125 ng/ml polymyxin B (P0972; Sigma-Aldrich) for two weeks and were analyzed six weeks post-irradiation.

For the adoptive transfer experiment, CD43 (Ly-48) MicroBeads (Miltenyi Biotec 130–097-148) were used to magnetically purify CD43$^-$ splenic B cells from naïve mice according to the manufacturer's instructions. Purified splenic B cells were stained with CD23-PE (B3B4, BioLegend), then CD23$^+$ cells were magnetically depleted, leaving a population of MZB. MZB were transferred into μMT host mice via intravenous injection into the tail.

For CreERT2-based deletion of LSD1, *Kdm1a*$^{fl/fl}$*Rosa26*$^{CreERT2/+}$ mice were treated with 40 mg total of tamoxifen. Tamoxifen powder (T5648; Sigma-Aldrich) was dissolved in corn oil previously described (10). Mice received daily injections i.p. for five days (8 mg per day). Following five additional days of rest, mice underwent experimental analysis.

Ex Vivo Development of Marginal Zone B Cells

OP9-DL1 and OP9-GFP mouse stromal cell lines (16) were obtained from Dr. Juan Carlos Zúñiga-Pflücker (University of Toronto). In a 24-well plate, 100,000 OP9-DL1 or OP9-GFP cells were plated in 1 ml of OP9 media (10 g/L α-MEM powder (12561; Thermo Fisher Scientific), 2.2 g/L sodium bicarbonate, pH 7.0, 5% heat-inactivated FBS, 1X penicillin/streptomycin).

CD93$^+$ cells were enriched from splenocytes from naïve mice by first staining cells with CD93-PE (AA4.1; BioLegend), then performing immunomagnetic enrichment of CD93-PE-stained cells with anti-PE microbeads (130–105-639; Miltenyi Biotec) according to the

manufacturer's instructions. Enriched cells were resuspended in B cell media (RPMI 1640, 10% heat-inactivated FBS, 0.05 mM 2-ME, 1X nonessential amino acids, 1X penicillin/streptomycin, 10 mM HEPES, and 1 mM sodium pyruvate) at 150,000 cells/ml, then 1 ml was plated onto OP9 cells after gently aspirating off OP9 media. 10 ng BAFF (8876-BF-010; R&D Systems) was added to the wells. Cells were placed in a 37°C incubator for 3 days, then underwent analyses. Where indicated, 800 nM of the IκB kinase inhibitor IKK-16 (Sigma SML1138) (17) or DMSO was added to the wells.

Flow Cytometry

Cells were resuspended at a concentration of 10^6 cells/100 μl fluorescence-activated cell sorting (FACS) buffer (1X PBS, 2 mM EDTA, 1% BSA). Cells were stained with Fc block (2.4G2; BD Biosciences) for 15 minutes, and then followed with specific Ab-fluorophores for one hour at 4°C, then washed with 10 volumes of FACS buffer. The following Abs or stains were used as indicated: B220-PE-Cy7 (RA3–6B2; Tonbo Biosciences), CD1d-BV605 (1B1; BD Biosciences), CD11b-APC-Cy7 (M1/70; Tonbo Biosciences), CD21-APC (B-ly4; BD Biosciences), CD23-eFluor450 (B3B4; eBioscience), CD43-PE (S7; BD Biosciences), CD45.1-FITC (A20; Tonbo Biosciences), CD45.2-PerCP-Cy5.5 (104; Tonbo Biosciences), CD90.2-APC-Cy7 (30-H12; BioLegend), CD93-PE (AA4.1), F4/80-APC-Cy7 (BM8; BioLegend), GL7-eFluor660 (GL-7; eBioscience), IgD-BV650 (IA6–2; BD Biosciences), IgM-FITC (II/41; eBioscience), Ly6A/E-PerCP-Cy5.5 (E13–161.7, BioLegend), Ly6C-PerCP-Cy5.5 (HK1.4, BioLegend), Zombie Yellow Fixable Viability Dye (kit no. 423104; BioLegend), and Live/Dead Fixable Blue Dead Cell Stain Kit for UV Excitation (L23105, Thermo Fisher Scientific). An LSRFortessa X-20 was used for analysis and a FACSAria II was used for sorting (BD Biosciences). All flow cytometry data were analyzed with FlowJo v9.9.5. Preceding all flow cytometry analyses presented is the following gating strategy: 1) lymphocytes (forward scatter [FSC]-area by side scatter [SSC]-area), 2) singlets (FSC-width by FSC-height), 3) singlets (SSC-width by SSC-height), 4) live cells (viability dye$^-$), 5) exclusion of non-B cell lineage cells (Thy1.1$^-$F4/80$^-$CD11b$^-$).

RNA-seq and Data Analysis

B220$^+$CD93$^-$GL7$^-$CD23$^-$CD21^{hi}CD1d$^+$ MZB and B220$^+$CD93$^-$GL7$^-$CD23$^+$CD21^{mid}CD1d$^-$ FoB were targeted to ensure pure, naïve populations. 50,000 cells were isolated via FACS into 600 μl RLT buffer (79216; Qiagen) containing 1% βME. Similarly, for transitional B cells (B220$^+$CD93$^+$) and *ex vivo*-derived MZB (B220$^+$CD21$^+$CD1d$^+$), 2,000 cells were isolated per sample via FACS into 300 μl RLT buffer as above. Cells were lysed by vortexing for one minute on high, and External RNA Controls Consortium (ERCC) spike-in RNA transcripts (18) were added (5 μl of 1:2000 dilution per sample) to enable downstream mRNA/cell calculations. Total RNA was isolated using a the Quick-RNA MicroPrep Kit (R1050; Zymo Research). For 50,000 cell preps, all RNA was used to create libraries with an mRNA HyperPrep Kit (KK8581; KAPA Biosystems). For 2,000 cell preps, all RNA was used to synthesize cDNA with the SMART-Seq v4 Ultra Low Input RNA Kit (Takara 634891) and libraries were generated with the Nextera XT DNA Library Prep Kit (Illumina FC-131–1096). An Agilent Bioanalyzer was used to quality control check each library. Libraries were pooled at an equimolar ratio and sequenced on a HiSeq 2500 system (Illumina) using 50 base pair paired-end chemistry.

Raw sequencing reads were mapped to the mm10 genome using STAR v2.2.1 (19). Gene counts were determined with the GenomicAlignments package v1.18.1 (20) using the mm10 transcriptome database. A gene was considered detected if all samples from a sample group had at least 0.1 mRNA/cell (the minimum ERCC transcript/cell concentration to detect at least 90% of that particular transcript across all samples) or one RPM. The edgeR package v3.24.3 (21) was used to determine differentially expressed genes based on both relative (false discovery rate (FDR) ≤ 0.05, no fold change cutoff) and absolute changes (FDR ≤ 0.05, no fold change cutoff) in expression as previously described (22). All differentially expressed genes (DEG) determined are listed in Supplemental Table 1. KEGG pathway analysis was performed with DAVID (23). Significance for DEG overlap comparisons was determined with Fisher's exact test. Observed/expected (obs/exp) ratios were calculated through permutation testing against gene sets randomly chosen from all detected genes (1,000 permutations per test). Significance for boxplot expression data was determined with Student's two-tailed *t*-test. PreRanked Gene Set Enrichment Analysis (GSEA) (24) was performed on all detected transcripts ranked based on the following equation:

$$\text{sign of fold change}(-\log_{10}(\text{edgeR } P \text{ value}))$$

ATAC-seq and Data Analysis

10,000 cells from the above cell types were isolated via FACS for ATAC-seq (25). Libraries were generated as described previously (26). Raw sequencing reads were mapped to the mm10 genome using Bowtie v1.1.1 (27). Peaks were called using MACS2 v2.1.1 (28) and annotated using HOMER v4.10 (29). Data were normalized to reads per peak per million (rppm) as previously described (30). A Benjamini-Hochberg FDR ≤ 0.05 and a fold change ≥ 1.5 was required for significance. All DAR determined are listed in Supplemental Table 2. Motif analysis was performed with the HOMER program findMotifsGenome.pl using randomly generated genomic sequences as background. PageRank analysis (31) was performed using raw ATAC-seq data and mRNA/cell gene expression data. Only transcription factors with a PageRank score >0.003 in at least one sample group of the indicated comparison were included to filter out less-important factors (corresponds to the top 10% of all transcription factors). Significance for boxplot enrichment data was determined with Student's two-tailed *t*-test.

qRT-PCR

Cells were pooled from six replicate cultures and $B220^+$ cells were enriched by first staining with B220-APC (RA3–6B2; Tonbo Biosciences), then performing immunomagnetic enrichment of B220-APC-stained cells with anti-APC microbeads (130–090-855; Miltenyi Biotec). 50,000 cells were added to 600 μl RLT buffer (Qiagen) containing 1% βME. Total RNA was isolated using a Quick-RNA MicroPrep Kit (R1050; Zymo Research) and reverse transcribed with SuperScript II Reverse Transcriptase (18064014; Invitrogen). cDNA was diluted 5-fold, and qPCR was performed with a CFX96 instrument (Bio-Rad Laboratories) using SYBR Green incorporation. Gene expression was calculated relative to 18S rRNA. Sequences for all primers are listed in Supplemental Table 3. Significance was determined with Student's two-tailed *t*-test.

Protein Purification

To quantify LSD1 protein levels in CKO and CreWT naïve B cells, $CD43^-$ splenic naïve B cells from both strains of mice were magnetically purified (Miltenyi Biotec 130–097-148) according to the manufacturer's instructions. Cells were washed in PBS, pelleted at 3,000 rpm for 5 minutes at 4°C, and were resuspended in 1X volume of cold RIPA buffer (20% glycerol, 50 mM Tris pH 8.0, 150 mM NaCl, 0.5% sodium deoxycholate, 0.1% SDS, 1% NP-40, 1 mM PMSF). Resuspended cells were put on ice for 20 minutes and centrifuged at 15,000 rpm for 10 minutes at 4°C. Resulting supernatant containing the protein was stored at −80°C.

Protein from the Raji human B cell line (32) either untreated or treated with 2 μg/ml α-CD40 antibody (5C3; BioLegend 334304) was isolated from nuclear and cytosolic fractions using a modified protocol (33). Cells were washed with cold PBS, washed with 5X volumes of hypotonic buffer (10 mM HEPES pH 7.9, 0.1 mM EDTA, 0.1 mM EGTA, 1.5 mM $MgCl_2$, 10 mM KCl, 1 mM DTT, 0.05% NP-40, 0.5 mM PMSF), resuspended in 3X volumes of hypotonic buffer, put on ice for 10 minutes, and homogenized by passing through an insulin syringe 5–10 times. A 0.1X volume of sucrose restore buffer (67.5% sucrose, 10 mM DTT, 1X sucrose restore buffer salts (10X sucrose restore buffer salts: 500 mM HEPES pH 7.9, 10 mM KCl, 2 mM EDTA)) was added and mixed by inverting 2–3 times. Nuclei were pelleted at 3,000 rpm for 5 minutes at 4°C. Supernatants were centrifuged at 15,000 rpm for 10 minutes at 4°C, and the resulting supernatant containing the cytoplasmic fraction was stored at −80°C until application.

For western blotting, nuclei were resuspended in 1X volume of cold RIPA buffer. Resuspended nuclei were put on ice for 20 minutes, sonicated for 30 seconds, centrifuged at 15,000 rpm for 10 minutes at 4°C, and the resulting supernatant containing the nuclear fraction was stored at −80°C. If the downstream application was co-immunoprecipitation, nuclei were resuspended in 5X volumes of cold IP lysis buffer (20 mM Tris pH 8.0, 135 mM NaCl, 20% glycerol, 1% NP-40, 1 mM PMSF, complete protease inhibitor cocktail (Sigma 05892970001)). Resuspended nuclei were rotated for 20 minutes at 4°C, centrifuged at 15,000 rpm for 10 minutes at 4°C, and the resulting supernatant containing the nuclear fraction was stored at −80°C.

Co-immunopreciptation

30 μl of Dynabeads M280 sheep anti-mouse IgG magnetic beads (11201D; Thermo Fisher Scientific) were washed 4X with 1 ml wash/binding buffer (PBS with 1% BSA) by rotating for 10 minutes at 4°C. 3 μg of primary antibody specific to LSD1 (B-9; sc-271720; Santa Cruz), p52/p100 (C-5; sc-7386; Santa Cruz), Lamin B (B-10; sc-374015; Santa Cruz), or control IgG (sc-2025; Santa Cruz) were bound to the beads overnight by rotating at 4°C. The beads were wash 2X in 1 ml wash/binding buffer, then mixed with 300 μg of protein extract in a final volume of 300 μl brought up with IP lysis buffer. Co-immunoprecipitation was performed by rotating for 3 hours at 4°C. Beads were washed 4X with 1 ml IP lysis buffer. Protein were eluted from beads by boiling for 10 minutes in Laemmli sample buffer with 5% βME and 100 mM DTT.

Western Blotting

Protein were resolved with SDS-PAGE, transferred to a PVDF membrane overnight, and probed with primary mouse anti-human antibodies diluted in TBS-T (150 mM NaCl, 20 mM Tris, 2 mM KCl, 0.1% Tween-20) containing 5% non-fat dry milk. Antibodies to the following were used: actin (AC-15; sc-69879; Santa Cruz; diluted 1:1000), LSD1 (diluted 1:400), p52/p100 (diluted 1:1,000), Lamin B (diluted 1:100), β-tubulin (D-10; sc-5274; Santa Cruz; diluted 1:100). Membranes were treated with a solution of HRP-conjugated sheep anti-mouse secondary antibody (A6782; Sigma) diluted 1:3,300 in TBS-T containing 5% non-fat dry milk and were visualized with the Chemi Hi Resolution application using a ChemiDoc MP imaging system (Bio-Rad laboratories).

Immunofluorescence

Spleens were prepared for staining as previously described (34). Slides were stained with a primary antibody cocktail of CD169-FITC (MOMA-1; MCA947F; Bio Rad Laboratories; diluted 1:50), IgM-Biotin (II/41; 553436; BD Biosciences; diluted 1:35), and CD1d (1B1; 123551; BioLegend; diluted 1:200) in serum blocking buffer. Slides were secondary stained with anti-FITC-A488 (polyclonal; A11090; Life Technologies; diluted 1:100) and streptavidin-Hilyte555 (60666; Anaspec; diluted 1:20) in serum blocking buffer. Slides were imaged on a Zeiss Axio Observer Z1 at room temperature with acquisition software Zen v2.0.0.0 (Blue Edition) using tiling and z-stacking. Images were taken with a 20X Plan-Apochromat 20x/0.8 objective (420650–9901; Zeiss) and an Axiocam 506 mono digital camera (Zeiss). Image files were analyzed with ImageJ v1.52k (NIH).

Results

LSD1 regulates marginal zone B cell development

LSD1 regulates B cell differentiation to plasma cells (10, 11), but its role in B cell development has not been explored. To examine its role from the pro-B to mature B cell stage, CD19-based B cell-conditional LSD1 deletion mice (CKO) (10) and *Cd19*$^{Cre/+}$ control mice (CreWT) were phenotyped by flow cytometry. Compared to CreWT mice, the bone marrow of CKO mice exhibited similar numbers of total B cells, pro-B cells, pre-B cells, immature B cells, and mature B cells (Fig. 1A–C). The spleen of CKO mice exhibited similar numbers of total B cells, transitional B cells, and FoB, but there was a 1.5-fold reduction in MZB (Fig. 1D–F). A significant reduction in MZB was also observed in CKO mice using two alternative MZB gating strategies (Fig. 1G–H). LSD1 protein was not detected in CKO splenic naïve B cells (Supplemental Fig. 1A), confirming knockout in this population. CKO and CreWT spleens were examined by immunofluorescence for markers IgM (total B cells), Cd1d (MZB), and CD169 (marginal zone macrophages) to determine if CKO splenic marginal zones were morphologically normal. Compared to CreWT, CKO spleens displayed characteristic marginal zone architecture outlined by CD169^{+} marginal zone macrophages (Fig. 2, green). White pulp regions also displayed normal patterns of IgM^{+} B cells and CD1d+ marginal zone B cells (Fig. 2, blue, red), suggesting that the decrease in CKO MZB is due to a developmental defect instead of a splenic architectural defect. B-1 B cell frequencies were assessed in the spleen and peritoneal cavity of CKO mice (Supplemental Fig. 1B–D). Both compartments exhibited a significant increase in B-1b cells

while the peritoneal cavity exhibited alterations in B-1 and B-2 population frequencies, suggesting that LSD1 regulates B-1 cell development. The ability of LSD1-deficient MZB to respond to the T-independent antigen LPS was examined by adoptively transferring CKO and CreWT MZB in a 1:1 ratio into B cell-deficient μMT host mice. CKO MZB exhibited a two-fold reduction in plasmablast formation (Supplemental Fig. 1E), verifying the known role that LSD1 has in regulating plasmablast differentiation (10).

To examine the intrinsic nature of CKO B-2 cell development, mixed bone marrow chimeras were established using an equal ratio of CD45.1 CKO and CD45.1/2 CreWT bone marrow in lethally-irradiated CD45.2 wild-type hosts. The frequencies and ratios of reconstituted host B cell compartments were analyzed with flow cytometry. MZB exhibited significantly lower frequencies of CKO cells compared to CreWT (Fig. 3A, B), which is reflected in a three- to four-fold reconstitution ratio favoring CreWT cells over CKO cells. Splenic FoB and T1 B cells exhibited similar reconstitution ratios between CreWT and CKO cells, but T2 B cells were skewed in favor of CreWT (Fig. 3A, C), supporting a defect in LSD1-deficient splenic B cell development. Lymph node B cells, pro-B cells, and bone marrow immature B cells also had similar frequencies; however, pre-B cells and bone marrow mature B cells displayed partially skewed reconstitution ratios (Fig. 3D–F). Overall, these data demonstrate that LSD1 regulates MZB development in a cell-intrinsic manner (Fig. 3G).

LSD1 functions as a transcriptional repressor in marginal zone B cells

The gene regulatory role that LSD1 plays in splenic B cell development was examined by performing RNA-seq on CKO and CreWT MZB and FoB. Principal component analysis (PCA) was performed on all 9,690 detected genes (Fig. 4A). Principal component 1 (PC1) stratified CreWT samples by cell type and MZB CreWT from CKO. PC2 further stratified MZB CKO from all samples. Intriguingly, FoB CreWT and CKO samples did not stratify by either PC component, indicating little transcriptional variation due to LSD deletion in those cell types. These data suggest that LSD1 regulates the MZB transcriptional program. Furthermore, the alignment of MZB CKO and FoB cell types suggests that MZB CKO transcriptomes possess FoB-like qualities.

To identify transcriptional differences between cell types and the effects of LSD deletion, differential gene expression analyses were performed on three sample group comparisons: MZB CreWT vs. FoB CreWT, FoB CKO vs. FoB CreWT, and MZB CKO vs. MZB CreWT (Fig. 4B). The comparison of MZB and FoB CreWT cells revealed that 1,887 genes that were significantly upregulated in MZB whereas only 101 genes were significantly upregulated in FoB, confirming that MZB and FoB possess distinct transcriptomes (8, 35). Known MZB genes were upregulated in MZB CreWT, including the homing receptor *S1pr1*, the transcription factor *Myc*, and the NOTCH2 target *Dtx1* (4, 6, 36). Similarly, known FoB genes were upregulated in FoB CreWT, including the homing receptors *Ccr7*, *Cxcr4*, and *Itgb7*, as well as the transcription factors *Bach2* and *Klf2* (5, 37, 38). Using GSEA (24), the data above were compared to two previous MZB studies (8, 35) (Supplemental Fig. 2A). Genes upregulated in MZB CreWT were significantly enriched for previously identified MZB genes while genes upregulated in FoB CreWT were significantly enriched for previously identified FoB genes, validating the datasets. Comparisons between CKO and

CreWT samples for each cell type identified 323 differentially expressed genes (DEG) between MZB CKO and MZB CreWT but only 48 DEG between FoB CKO and FoB CreWT, supporting the conclusion from the PCA that LSD1 primarily regulates the MZB transcriptome. MZB CKO had 297 up DEG and only 26 down DEG, suggesting that LSD1, similar to plasmablasts and germinal center B cells (10, 11), mainly plays a repressive role in regulating MZB transcription.

DEG across all samples were assessed and organized based on function (Fig. 4C). Signaling genes upregulated in MZB CKO that are known to play a role in B cell development included *Cdkn2c* and *Flt3*. CDKN2C is a cyclin-dependent kinase inhibitor that suppresses cell cycle G1 progression and is known to regulate splenic B cell homeostasis (39). Loss of FLT3-ligand in mice results in a cell extrinsic increase in MZB and decrease in FoB, suggesting an important role for FLT3 signaling in splenic B cell development (40). Genes encoding transcriptional regulators important for B cell development were overexpressed in MZB CKO. These included the transcription factors BACH2 and BCL6, which are critical for bone marrow B cell development (37); ID3, which promotes MZB formation by inhibiting basic helix-loop-helix transcription factors such as E2A (41); and IRF1 and IRF7, which regulate the expression of interferon response genes (42). Genes encoding surface proteins involved in adhesion and migration were upregulated as well and included *Cxcr4* and *Itgb7*, which facilitate homing to the bone marrow and gut, respectively (5). These two genes exhibited a significant increase in surface expression on MZB (Supplemental Fig. 2B,C), validating the gene expression data. BACH2 and BCL6 are also known to promote germinal center B cell formation (43), but there was no significant increase in germinal center B cells in CKO spleens (Supplemental Fig. 2D).

Genes critical for FoB function such as *Klf2*, *Bach2*, *Itgb7*, and *Cxcr4* were upregulated in MZB CKO, implying defective MZB development through aberrant expression of FoB genes. To further explore this effect, the top 200 significant genes upregulated in FoB CreWT compared to MZB CreWT were analyzed for enrichment in MZB CKO genes using GSEA (Fig. 4D). The results displayed a significant enrichment of FoB CreWT genes in the MZB CKO cells. Furthermore, the 297 up DEG in MZB CKO were tested for significant overlap with the 101 up DEG in FoB CreWT (Fig. 4E). A total of 56 genes overlapped between the two groups, which was 18.3-fold more than expected by chance. Additional example FoB genes include those that encode JUND, a transcription factor that promotes *Bcl6* expression in germinal center B cells (44), CD200, a receptor that is overexpressed on B cell neoplasms and regulates anti-tumor immunity (45), and IL21R, which binds IL-21 to regulate B cell proliferation, differentiation, and survival (46). Also, because some MZB CKO upregulated DEG are highly expressed in myeloid cells, such as *Csf2ra*, *Irf1*, *Irf7*, and *Itgam*, and pre-B cells can be transdifferentiated into macrophages by altering the pre-B cell transcriptional network (47), MZB CKO genes were tested for enrichment of myeloid progenitor (48) and macrophage lineage (49) genes (Supplemental Fig. 2E). MZB CKO were significantly enriched for these gene sets, suggesting that in the absence of LSD1, there is lineage dysregulation into a myeloid-type cell. Thus, LSD1 is important for establishing the transcriptional identity of MZB during splenic B cell development, partly through repressing FoB and myloid lineage transcriptional programs.

LSD1 represses chromatin accessibility at NF-κB motifs

The effect that LSD1 deficiency has on chromatin accessibility in FoB and MZB was addressed by performing ATAC-seq on the same sample groups as RNA-seq. PCA on all 94,161 peaks showed that samples separated by both cell type and LSD1 deletion status (Fig. 5A). MZB CKO samples separated more from MZB CreWT samples by PC2 compared with the separation between FoB CKO and CreWT samples, suggesting that LSD1 has a larger impact on chromatin accessibility in MZB than FoB.

Differential accessibility analysis was performed on three sample group comparisons: MZB CreWT vs. FoB CreWT, FoB CKO vs. FoB CreWT, and MZB CKO vs. MZB CreWT (Fig. 5B). Comparison of FoB CreWT and MZB CreWT revealed thousands of differentially accessible regions (DAR), indicating that these cell types are very distinct at the level of chromatin accessibility. Compared to their CreWT counterparts, MZB CKO had 1,014 total DAR while FoB CKO had 678 total DAR, with DAR increasing in accessibility being more numerous than DAR decreasing in accessibility for both comparisons. Thus, LSD1 regulates chromatin accessibility in both MZB and FoB – but to a greater extent in MZB – and plays more of a repressive role in both cell types.

To understand what transcription factor binding motifs were enriched within DAR, motif enrichment analysis was performed and enrichment *P* values for top motifs were plotted as a heatmap for the CreWT, FoB CKO, and MZB CKO sample group comparisons (Fig. 5C, D, Supplemental Fig. 3A). For the MZB and FoB CreWT comparison (Fig. 5C), ETS factor motifs were highly enriched in both DAR groups. ETS factors such as SPIB, SPI1, ETS1, and FLI1 are known to regulate splenic B cell development (50–52) and may be influencing chromatin accessibility in these cell types. Transcription factor binding motifs for bHLH, POU, Rel homology domain (RHD), and RUNT factors were more enriched in MZB CreWT DAR, suggesting a role for these factors in regulating MZB chromatin accessibility. Certain bHLH factors such as TCF3 (E2A), TCF4 (E2–2), and MYC regulate the formation and function of splenic B cells (6, 41, 53). Both POU factors and RHD factors are required for normal splenic B cell development (54–56). IRF and KLF factor motifs were more enriched in FoB CreWT DAR. Since KLF2 and IRF4 activate genes important for follicular B cell function (38, 42), they may influence chromatin accessibility to exert their transcriptional regulation.

For the CreWT vs. CKO comparisons (Fig. 5D, Supplemental Fig. 3A), ETS factor motifs were highly enriched in all DAR groups. LSD1 has been shown to modulate chromatin accessibility at ETS motifs and binding sites in plasmablasts or a B cell line (10, 57), providing further evidence for B cell-specific LSD1-based regulation at these sites. MZB CKO up DAR were enriched for CTCF, KLF, RHD, and RUNT binding motifs, whereas MZB CreWT DAR were enriched for bHLH, GATA, HSF, and POU binding motifs. LSD1 has been shown to interact directly with the bHLH factors MYOD and TAL1 (58, 59) and the RHD factor p65 (60), supporting the possibility that LSD1 may cooperate with transcription factors of the same families during B cell development to exert its effects on chromatin accessibility and gene expression.

PageRank analysis was used to integrate RNA-seq data and ATAC-seq data to rank transcription factors in each sample group by predicted importance based on the expression and identity of its target genes (31). The PageRank score of the top 20 transcription factors (out of 639 analyzed) per sample group were plotted as a heatmap (Supplemental Fig. 3B). Reflecting their shared precursor origins, the analysis indicated that FoB and MZB share many top factors, including SPIB, ETS1, ELF1, p50, and p52. Some transcription factors are unique to certain sample groups, such as PBX2 to MZB, indicating a more prominent role in target gene regulation for these factors in these sample groups.

PageRank between MZB CreWT and FoB CreWT (Fig. 5E) identified factors known to be important for the formation and function of MZB and/or FoB were identified and include BACH2, BCL6, EBF1, FLI1, MYC, p52, and TCF4 (6, 37, 52, 53, 55, 61). Other factors identified such as MEIS3 and PBX2 have not been shown to play a role in B cell development, but are known to regulate the development of other cell types (62, 63). Between FoB CKO and FoB CreWT, transcription factors such as NF-κB p52 were determined to be more important in FoB CKO despite the relatively unchanged FoB CKO transcriptome and lack of a splenic FoB phenotype in CKO mice. Between MZB CKO and MZB CreWT, the transcription factors BACH2, CIC, EBF1, p52, STAT6, and TCF3 were determined to be more important to the MZB CKO transcriptional program, implying LSD1-dependent regulation of their downstream target genes.

The transcription factors most likely to cooperate with LSD1 to directly regulate target genes through modulation of chromatin accessibility were determined by filtering MZB CKO by PageRank score (> 0.5 or < -0.5), and then analyzing filtered transcription factors for 1) highest percent DEG of all target regulated genes, and 2) chromatin accessibility changes at motifs mapping to these DEG. EBF1, p52, and STAT6 had the highest percent of MZB CKO DEG of their target regulated genes (Supplemental Fig. 3C). Of these factors, only p52 exhibited a significant increase in accessibility in MZB CKO compared to MZB CreWT (Supplemental Fig. 3D), suggesting that without LSD1, p52 fails to properly repress target gene expression and chromatin accessibility, possibly through a direct interaction.

The biological roles of transcription factors were explored by examining their PageRank-determined target genes. PBX2, which was identified as important in MZB CreWT compared to FoB CreWT, is not known to have a role in B cell development. Here, PBX2 was predicted to upregulate 59 DEG in MZB CreWT that were determined to be involved in a number of processes via KEGG pathway analysis, the most significant being carbon metabolism and mismatch repair (Supplemental Fig. 3E). Example genes include the metabolic enzymes *Got1*, *H6pd*, and *Prps2* and the DNA repair enzymes *Mlh1* and *Rpa3*. These data suggest a novel role for PBX2 in marginal zone B cell function. In MZB CKO, EBF1 was predicted to have a dysregulated transcriptional network upon LSD1 deletion despite not having dysregulated chromatin accessibility at target motifs, suggesting an indirect LSD1-mediated regulatory effect. EBF1 is known to regulate genes involved in the B cell receptor signaling pathway and does so in an LSD1-dependent manner with the genes *Pik3cg* and *Rasgrp3* (Supplemental Fig. 3F), suggesting a possible role for LSD1 in regulating this process (61). p52 was predicted to upregulate 23 DEG in MZB CKO, including the transcriptional regulators BACH2 and ID3, the receptors S100a10 and TLR2,

and the signaling molecules PIK3CG, RASGRP3, and SPATA13 (Fig. 5F). p52 binding motifs were assessed individually for overlap with DAR. Four of these were identified in the p52-target DEGs *Crisp3*, *Id3*, *S100a10, and Sapcd1* (Fig. 5G and Supplemental Fig. 3G). Nineteen other p52 motif-containing DAR were located throughout the genome (Supplemental Fig. 3H). In addition to the above, 10 DAR that did not contain a p52 motif mapped to p52-target DEG (*Setbp1* and *Tlr2*) (Supplemental Fig. 3I). Together, these data suggest a role for LSD1 in directly repressing the expression of p52-target genes by limiting chromatin accessibility at p52 binding sites.

LSD1 regulates ex vivo marginal zone B cell development induced by NOTCH2 and non-canonical NF-κB signaling

The above analysis suggested a dependence of LSD1 on non-canonical NF-κB signaling through p52, a critical factor for MZB formation (54). To assess the relevance of LSD1 in non-canonical NF-κB signaling during MZB development CKO and CreWT $B220^+CD93^+$ transitional stage B cells (TrB) were cultured on OP9-DL1 cells, which stimulate NOTCH2 signaling through delta-1 ligand expression; and in the presence of BAFF to stimulate non-canonical NF-κB signaling (1). Pre-cultured TrB displayed similar population levels between CKO and CreWT mice and exhibited low surface expression of the MZB surface markers CD21 and CD1d (Fig. 6A, B). After 3 days in culture, 14–20% of all CreWT TrB developed into $B220^+CD21^+CD1d^+$ *ex vivo*-derived MZB (eMZB), whereas only 6–10% of CKO TrB developed into eMZB (Fig. 6C). Cells were developed under additional conditions, including controls for BAFF and the delta-1 ligand DL1 (Supplemental Fig. 4A). LSD1-deficient cells developed into significantly fewer MZB under all conditions, suggesting a defect in both NOTCH2 and non-canonical NF-κB signaling. To ensure that the defect was due to the absence of LSD1 in splenic B cell development and not earlier stages, $Kdm1a^{fl/fl}Rosa26^{CreERT2/+}$ (IKO) and $Kdm1a^{fl/fl}Rosa26^{+/+}$ (WT) $CD93^+$ TrB were cultured *ex vivo* as above at day five after tamoxifen treatment (Fig. 6D, Supplemental Fig. 4B). The same defect was observed, indicating that the reduction in eMZB CKO cells is likely due to a defect in splenic B cell development.

To determine whether LSD1 regulated NOTCH2-target and/or NF-κB-target genes during eMZB development, RNA-seq was performed on LSD1-deficient and -sufficient eMZB and TrB. PCA indicated that TrB CreWT stratified from eMZB CreWT but not eMZB CKO (Fig. 6E), suggesting that changes induced by NOTCH2 and/or NF-κB signaling normally observed in eMZB CreWT are not occurring in eMZB CKO. Minimal stratification was observed between TrB CKO and TrB CreWT, indicating that LSD1 does not have a strong role in regulating the TrB transcriptional program. Differential expression analysis was performed on the indicated sample groups (Fig. 6F). The 3,220 total DEG observed between TrB CreWT and eMZB CreWT showed that the two cell types were transcriptionally distinct, with eMZB CreWT upregulating MZB genes such as *Myc*, *Dtx1*, and *S1pr1* and TrB CreWT upregulating transitional B cell genes such as *Myb* and *Sox4*. Using GSEA, MZB genes from this study and two others (8, 35) were shown to be significantly enriched in eMZB CreWT genes (Fig. 6G, Supplemental Fig. 4C), validating the *ex vivo* MZB development assay as a viable method for testing MZB development. CKO comparisons showed 46 total changes in gene expression between TrB CKO and TrB CreWT and 108

total changes in gene expression between eMZB CKO and eMZB CreWT, with most changes being increases (Fig. 6F). eMZB CKO genes, but not TrB CKO genes, were significantly enriched for MZB genes (Fig. 6H). Additionally, 30 out of the 72 eMZB CKO upregulated DEG overlapped the 297 MZB CKO upregulated DEG (Fig. 6I, 11.1-fold more than expected by chance), including homing receptors *Cxcr4* and *Itgb7*. These data further support a repressive role for LSD1 during MZB development and suggest a similar role for LSD1 during both *in vivo* and *ex vivo* MZB development.

MZB CKO and eMZB CKO genes were tested for enrichment in NOTCH2 and NF-κB target genes, which were acquired from the Molecular Signatures Database (MSigDB) (64) and, in the case of NF-κB target genes, the PageRank analysis from this study and publications involving genetic deletion of NF-κB signaling transcription factors (54, 55, 65–67). NOTCH2 target genes were not significantly enriched in MZB CKO or eMZB CKO (Supplemental Fig. 4D). Of all 21 NF-κB target gene sets tested, seven gene sets were significantly enriched in MZB CKO while four gene sets were significantly enriched in eMZB CKO (Supplemental Fig. 4E). Of these sets, two were enriched in both MZB CKO and eMZB CKO and represent genes abberantly upregulated when either *Nfkb2* or *Relb* are deleted in splenic naïve B cells treated with BAFF. Importantly, genes upstream of both NOTCH2 signaling and NF-κB signaling, such as *Notch2* and the BAFF receptor (*Tnfrsf13c*), were not dysregulated in MZB CKO, TrB CKO, or eMZB CKO (Supplemental Fig. 4F). Thus, in the absence of LSD1, these data suggest a defect in the expression of non-canonical NF-κB signaling target genes, but not NOTCH2 signaling target genes.

LSD1 and NF-κB cooperate to regulate marginal zone B cell development

Genes regulated by both LSD1 and NF-κB signaling were further analyzed to understand how LSD1 and NF-κB intersect. Of the genes encoding transcription factors that form a functional NF-κB complex, *Nfkb2*, *Rela*, *Relb*, and *Rel* are induced in eMZB compared to TrB while *Nfkb1* is not (Fig. 7A), implying that p50 complexes play a lesser role in *ex vivo* MZB development than p52 complexes. This is further supported by the finding that of all p50 and p52 target genes from PageRank analysis and GSEA gene sets used above (Supplemental Fig. 4G), eMZB express 70% of all p52 genes while they only express 42% of all p50 genes (Supplemental Fig. 4H). Genes regulated by p52 complexes in splenic naïve B cells treated with BAFF (54, 55) or predicted to be regulated by p52 by PageRank analysis were examined for gene expression changes in MZB CKO and eMZB CKO. A total of 37 genes that were DEG in both sample groups or were a DEG in one group and trending up in the other group are displayed (Fig. 7B). Genes include those that encode PTPRV, a protein tyrosine phosphatase that mediates p53-induced cell cycle exit (68), CSRP1, a LIM-domain protein that suppresses cell proliferation and development (69), Ly6A, a surface protein that promotes hematopoietic stem cell development and survival (70), CDH17, a cadherin that regulates early B cell development (71), and ID3, a transcription factor that promotes MZB formation (41). Total expression of these 37 genes in both MZB CKO and eMZB CKO were significantly higher than their CreWT counterparts (Fig. 7C). Additionally, p52 motifs mapping to these genes exhibit a significant increase in chromatin accessibility in MZB CKO, supporting that they are repressed by LSD1 (Fig. 7D).

Non-canonical NF-κB signaling through the transcription factors p52 and RelB is critical for splenic B cell development, as indicated by B cell-conditional knockout of *Nfkb2* and *Relb* (55). To confirm the role of non-canonical NF-κB signaling during *ex vivo* MZB development, the NF-κB inhibitor IKK-16 (17) was applied to *ex vivo* MZB cultures of C57BL/6 wild-type cells (Supplemental Fig. 4I). Cultures treated with 800 nM of IKK-16 exhibited a significant decrease in eMZB compared to control cells treated with DMSO, showing that non-canonical NF-κB signaling is critical for *ex vivo* MZB development and suggesting that both inhibition of NF-κB signaling and LSD1 deficiency affect a similar pathway. To assess pathway overlap, LSD1-deficient cultures were treated with IKK-16 (Fig. 7E). CKO inhibitor cultures exhibited a significant decrease in eMZB compared to both CKO DMSO cultures and CreWT inhibitor cultures, but this decrease was not completely additive. These data imply a degree of overlap between pathways affected by both LSD1 deletion and NF-κB inhibition.

To confirm that genes from Fig. 7B are regulated by both LSD1 and NF-κB signaling, RNA was collected from B cells from the four culture conditions displayed in Fig. 7E (Supplemental Fig. 4J) and RT-qPCR was performed to assess the expression of the nine genes that are DEG in both MZB and eMZB (*Csrp1*, *Ehd2*, *Eno1b*, *Il2ra*, *Ly6c2*, *Padi2*, *Pqlc1*, *Ptprv*, *Spata13*). The genes *Ccr7*, *JunB*, and *Tap1*, which are known targets of canonical NF-κB signaling (72–74), were used as negative controls. RT-qPCR revealed that the genes *Csrp1*, *Il2ra*, *Ly6c2*, *Padi2*, *Ptprv*, and *Spata13* were significantly upregulated in CreWT inhibitor cultures compared to CreWT DMSO cultures, indicating their repression by NF-κB signaling (Fig. 7F). The six significant genes from above plus the gene *Ehd2* were significantly upregulated in CKO inhibitor cultures relative to CreWT DMSO cultures, indicating possible pathway overlap. The three conical NF-κB signaling genes were not differentially expressed in any condition, supporting that the gene dysregulation observed is due to a defect only in non-canonical NF-κB signaling. Flow cytometry was used to validate the surface expression of Ly6A, which was found to be significantly increased upon LSD1 deletion and NF-κB inhibition (Fig. 7G).

Endogenous interaction of LSD1 with p52 was examined by co-immunoprecipitation experiments performed in the Raji human B cell line (32), from which sufficient quantities of protein could be obtained. To induce p52 nuclear translocation, Raji cells were treated with anti-CD40 Ab, and nuclear and cytoplasmic fractions were assessed (Fig. 7H). At four hours post-treatment, nuclear p52 levels increased while its cytoplasmic precursor p100 levels decreased, indicating that anti-CD40 Ab treatment successfully stimulated p52 nuclear translocation. Co-immunoprecipitation of p52 and LSD1 was performed on Raji nuclear lysate at four days post anti-CD40 Ab treatment (Fig. 7I). LSD1 immunoprecipitated with p52 and p52 immunoprecipitated with LSD1, indicating that the two proteins are found within the same complex. Together, these data confirm a critical regulatory role for non-canonical NF-κB signaling and demonstrate a cooperative relationship between this signaling pathway and LSD1 in MZB development.

Discussion

This study establishes a clear role for LSD1 in MZB development and begins to define the epigenetic mechanisms that govern splenic B cell development. LSD1 promoted MZB formation and functioned to repress gene expression in both *in vivo*- and *ex vivo*-generated MZB. LSD1 also regulated chromatin accessibility in MZB at motifs of transcription factors that are critical for splenic B cell development, including NF-κB. Bioinformatic analyses of RNA-seq and ATAC-seq data pointed towards LSD1 having a major regulatory effect on p52-target genes and p52 motifs that mapped to these genes. Experiments involving the application of an NF-κB inhibitor to *ex vivo* MZB development indicated pathway overlap between LSD1 and non-canonical NF-κB signaling. The presence of LSD1 and p52 in the same complex further demonstrated cooperation between a DNA binding protein and an epigenetic modifier to drive the bifurcation of the development of the MZB and FoB cell fates.

MZB and FoB display hundreds of differentially expressed genes, many of which have been shown to guide their development and give rise to their unique cellular attributes (1, 2). This study begins to reveal the epigenetic mechanisms behind these differences in gene expression and defines LSD1 as a critical epigenetic regulator for a subset of MZB-specific genes. LSD1 represses multiple genes that are typically upregulated in FoB, including those that encode the key FoB transcription factor KLF2 and its target migratory surface receptors CXCR4 and ITGB7 (5, 38). Regardless of regulating these genes, CKO MZB localize normally in the splenic marginal zone (Fig. 2). LSD1 also represses the genes that encode the Blimp-1 repressors BACH2 and BCL6 (37), suggesting that CKO MZB may respond poorly to antigen. Although MZB generate plasmablasts in response to TLR agonists in a Blimp-1-dependent manner (75), the response of LSD1-deficient MZB to the TLR4 agonist LPS has been observed to be significantly defective due in part to LSD1 regulating Blimp-1 target genes and other key plasmablast genes (10). Based on this observation, it will be difficult to discern the extent to which LSD1-target genes that are dysregulated during MZB development, such as *Bach2* and *Bcl6*, actually contribute to MZB differentiation. Despite lack of evidence for an LSD1-specific role in MZB function, it is clear that LSD1 promotes the BAFF-initiated p52-dependent development of TrB into MZB. p52-target genes significantly upregulated in both CKO MZB and eMZB represent the highest-confidence genes that contribute to the observed decrease in MZB development and include the regulators of lymphocyte proliferation and development *Ptprv*, *Csrp1*, *Ly6a*, *Cdh17*, and *Id3* (41, 68–71). Of these genes, *Id3* is particularly critical for MZB formation, and although deletion of *Id3* results in fewer MZB (41), the effect of *Id3* overexpression has not been studied in the context of splenic B cell development. Even though it was previously shown that LSD1-deficient naïve B cells globally downregulate cell cycle genes and exhibit decreased proliferation in response to LPS (10), no cell cycle genes were downregulated in CKO MZB or eMZB, implying a different mechanism for LSD1-dependent MZB development. Furthermore, dozens of additional genes associated with multiple pathways are dysregulated in LSD1-deficient MZB *in vivo* compared to *ex vivo*, suggesting that LSD1 may regulate MZB developmental pathways aside from BAFF-induced non-canonical NF-κB signaling. PageRank data suggested that LSD1 regulates EBF1-target genes associated

with B cell receptor signaling (Fig. 5E, Supplemental Fig. 2F). This process is critical for the bifurcation of TrB into MZB and FoB and may represent either a direct or indirect LSD1 target pathway that influences splenic B cell development.

NF-κB transcription factors have been shown to influence the epigenome (76, 77), but not in the context of B cell development. The data presented here strongly implies regulation of p52-target genes by LSD1 in MZB. In macrophages, LSD1 directly interacts with and demethylates p65 to stabilize it and amplify the inflammatory response to LPS (60). It is possible that LSD1 demethylates a component of the NF-κB heterodimers that form downstream of non-canonical NF-κB signaling, resulting in the altered epigenome and transcriptome observed in MZB CKO. However, given that LSD1 demethylates H3K4me1 in plasmablasts and germinal center B cells (10, 11), it is also possible that LSD1 is functioning with non-canonical NF-κB transcription factors to demethylate surrounding H3K4 residues to repress target genes. This function is supported by the predominantly repressive role that LSD1 has in MZB in regulating transcription and chromatin accessibility. A similar effect has been observed with the LSD1 homologue LSD2, as it can interact with c-Rel to demethylate promoter-based chromatin (78).

The finding that B cell conditional deletion of LSD1 impairs MZB development but not FoB development raises questions as to how LSD1 selectively affects one cell fate over another. LSD1 is only modestly upregulated in MZB compared to FoB (Fig. 3A), suggesting that strict abundance of mRNA and potentially protein levels are not likely the major mechanism. All five NF-κB family member genes are expressed similarly in MZB and FoB. Thus, no NF-κB transcription factor is present only in MZB to facilitate LSD1-dependent gene regulation. Genes expressed exclusively by MZB may be influencing NF-κB-based LSD1 activity. For example, the non-canonical IKK kinase IKKε promotes gene regulatory capabilities of a p52-p65 NF-κB complex (79) and is significantly upregulated in MZB compared to FoB (8), suggesting increased p52 activity in MZB. The high expression of both *Nfkb2* and *Rela* in eMZB (Fig. 6A) in addition to previous work showing that both p52 and p65-based NF-κB complexes are capable of repressing genes through epigenetic mechanisms (80, 81) support the possibility of a p52-p65 complex functioning with LSD1 as a transcriptional repressor during MZB development. Also, because cell signaling is known to drive cell fate bifurcation in other hematopoietic developmental pathways (82, 83), it is possible that gene programs induced by NOTCH2 signaling may be influencing LSD1-based selectivity.

The epigenetic reprogramming of lymphocytes during development is crucial for proper immune system formation and function (84). Developing B cells in the bone marrow exhibit distinct patterns of chromatin accessibility and histone modifications (85), and this study demonstrates that the epigenome remains dynamic throughout splenic B cell development as well. Therapeutic targeting of histone modifying enzymes is used to treat numerous hematopoietic malignancies (86, 87), and the data presented here support that malignancies arising from splenic B cell development, such as marginal zone B cell lymphomas (88), can be targeted as well. Overall, this study defines LSD1 as a novel epigenetic regulator of splenic B cell development, identifies cooperation between LSD1 and non-canonical NF-κB

signaling in regulating downstream MZB genes, and expands our knowledge of the epigenetic regulation of B cell development.

Supplementary Material

Refer to Web version on PubMed Central for supplementary material.

Acknowledgements

We acknowledge members of the Boss lab for scientific contributions and editorial input. We specifically thank Royce Butler for animal husbandry contributions, Dillon Patterson for ATAC-seq tagmentation, and Sakeenah Hicks for sequencing library preparations. We thank the Emory Flow Cytometry Core for FACS, the Emory Integrated Genomics Core for sequencing library QC, and the NYU Genome Technology center for Illumina sequencing. We thank Dr. Mahmood Mohtashami and Dr. Juan Carlos Zúñiga-Pflücker of the University of Toronto for providing the OP9-DL1 and OP9-GFP cell lines. We thank Dr. Wasif Kahn of the University of Miami for sharing his transcriptomics data from MZB and FoB.

This work was supported by the following NIH grants: R01 AI123733 and P01 AI125180 to J.M.B., T32 GM0008490 to R.R.H., and F31 AI131532 to R.R.H.

Abbreviations

ATAC-seq	assay for transposase-accessible chromatin sequencing
CKO	*Kdm1a*$^{fl/fl}$ *Cd19*$^{Cre/+}$ conditional knockout
CreWT	*Kdm1a*$^{+/+}$ *Cd19*$^{Cre/+}$ wild-type
DAR	differentially accessible region
DEG	differentially expressed gene
ERCC	external RNA controls consortium
FACS	fluorescence-activated cell sorting
FC	fold change
FDR	false discovery rate
FoB	follicular B cell
FSC	forward scatter
GSEA	gene set enrichment analysis
H3K4me1	histone 3 lysine 4 monomethylation
H3K4me2	histone 3 lysine 4 dimethylation
H3K27me3	histone 3 lysine 27 trimethylation
H3K9me1	histone 3 lysine 9 monomethylation
H3K9me2	histone 3 lysine 9 dimethylation
IKO	*Kdm1a*$^{fl/fl}$ *Rosa26*$^{CreERT2/+}$ inducible knockout

LPS	lipopolysaccharide
LSD1	lysine-specific demethylase 1
MZB	marginal zone B cell
nB	naïve B cells
PB	plasmablasts
PC	plasma cells
PCA	principal component analysis
qPCR	quantitative polymerase chain reaction
qRT-PCR	quantitative reverse transcription PCR
rpm	reads per million
rppm	reads per peak per million
SD	standard deviation
SSC	side scatter
TrB	transitional B cel
WT	*Kdm1a*$^{fl/fl}$ wild-type

References

1. Pillai S, and Cariappa A 2009 The follicular versus marginal zone B lymphocyte cell fate decision. Nat Rev Immunol 9: 767–777. [PubMed: 19855403]
2. Cerutti A, Cols M, and Puga I 2013 Marginal zone B cells: virtues of innate-like antibody-producing lymphocytes. Nat Rev Immunol 13: 118–132. [PubMed: 23348416]
3. Niiro H, and Clark EA 2002 Regulation of B-cell fate by antigen-receptor signals. Nat Rev Immunol 2: 945–956. [PubMed: 12461567]
4. Cinamon G, Matloubian M, Lesneski MJ, Xu Y, Low C, Lu T, Proia RL, and Cyster JG 2004 Sphingosine 1-phosphate receptor 1 promotes B cell localization in the splenic marginal zone. Nat Immunol 5: 713–720. [PubMed: 15184895]
5. Campbell DJ, Kim CH, and Butcher EC 2003 Chemokines in the systemic organization of immunity. Immunol Rev 195: 58–71. [PubMed: 12969310]
6. Meyer-Bahlburg A, Bandaranayake AD, Andrews SF, and Rawlings DJ 2009 Reduced c-myc expression levels limit follicular mature B cell cycling in response to TLR signals. J Immunol 182: 4065–4075. [PubMed: 19299704]
7. Rubtsov AV, Swanson CL, Troy S, Strauch P, Pelanda R, and Torres RM 2008 TLR agonists promote marginal zone B cell activation and facilitate T-dependent IgM responses. J Immunol 180: 3882–3888. [PubMed: 18322196]
8. Kleiman E, Salyakina D, De Heusch M, Hoek KL, Llanes JM, Castro I, Wright JA, Clark ES, Dykxhoorn DM, Capobianco E, Takeda A, Renauld JC, and Khan WN 2015 Distinct Transcriptomic Features are Associated with Transitional and Mature B-Cell Populations in the Mouse Spleen. Front Immunol 6: 30. [PubMed: 25717326]
9. Maiques-Diaz A, and Somervaille TC 2016 LSD1: biologic roles and therapeutic targeting. Epigenomics 8: 1103–1116. [PubMed: 27479862]

10. Haines RR, Barwick BG, Scharer CD, Majumder P, Randall TD, and Boss JM 2018 The Histone Demethylase LSD1 Regulates B Cell Proliferation and Plasmablast Differentiation. J Immunol 201: 2799–2811. [PubMed: 30232138]
11. Hatzi K, Geng H, Doane AS, Meydan C, LaRiviere R, Cardenas M, Duy C, Shen H, Vidal MNC, Baslan T, Mohammad HP, Kruger RG, Shaknovich R, Haberman AM, Inghirami G, Lowe SW, and Melnick AM 2019 Histone demethylase LSD1 is required for germinal center formation and BCL6-driven lymphomagenesis. Nat Immunol 20: 86–96. [PubMed: 30538335]
12. Rickert RC, Roes J, and Rajewsky K 1997 B lymphocyte-specific, Cre-mediated mutagenesis in mice. Nucleic Acids Res 25: 1317–1318. [PubMed: 9092650]
13. Wang J, Scully K, Zhu X, Cai L, Zhang J, Prefontaine GG, Krones A, Ohgi KA, Zhu P, Garcia-Bassets I, Liu F, Taylor H, Lozach J, Jayes FL, Korach KS, Glass CK, Fu XD, and Rosenfeld MG 2007 Opposing LSD1 complexes function in developmental gene activation and repression programmes. Nature 446: 882–887. [PubMed: 17392792]
14. Otero DC, Anzelon AN, and Rickert RC 2003 CD19 function in early and late B cell development: I. Maintenance of follicular and marginal zone B cells requires CD19-dependent survival signals. J Immunol 170: 73–83. [PubMed: 12496385]
15. Ventura A, Kirsch DG, McLaughlin ME, Tuveson DA, Grimm J, Lintault L, Newman J, Reczek EE, Weissleder R, and Jacks T 2007 Restoration of p53 function leads to tumour regression in vivo. Nature 445: 661–665. [PubMed: 17251932]
16. Holmes R, and Zuniga-Pflucker JC 2009 The OP9-DL1 system: generation of T-lymphocytes from embryonic or hematopoietic stem cells in vitro. Cold Spring Harb Protoc 2009: pdb prot5156.
17. Waelchli R, Bollbuck B, Bruns C, Buhl T, Eder J, Feifel R, Hersperger R, Janser P, Revesz L, Zerwes HG, and Schlapbach A 2006 Design and preparation of 2-benzamido-pyrimidines as inhibitors of IKK. Bioorg Med Chem Lett 16: 108–112. [PubMed: 16236504]
18. Jiang L, Schlesinger F, Davis CA, Zhang Y, Li R, Salit M, Gingeras TR, and Oliver B 2011 Synthetic spike-in standards for RNA-seq experiments. Genome Res 21: 1543–1551. [PubMed: 21816910]
19. Dobin A, Davis CA, Schlesinger F, Drenkow J, Zaleski C, Jha S, Batut P, Chaisson M, and Gingeras TR 2013 STAR: ultrafast universal RNA-seq aligner. Bioinformatics 29: 15–21. [PubMed: 23104886]
20. Lawrence M, Huber W, Pages H, Aboyoun P, Carlson M, Gentleman R, Morgan MT, and Carey VJ 2013 Software for computing and annotating genomic ranges. PLoS Comput Biol 9: e1003118. [PubMed: 23950696]
21. Robinson MD, McCarthy DJ, and Smyth GK 2010 edgeR: a Bioconductor package for differential expression analysis of digital gene expression data. Bioinformatics 26: 139–140. [PubMed: 19910308]
22. Barwick BG, Scharer CD, Bally APR, and Boss JM 2016 Plasma cell differentiation is coupled to division-dependent DNA hypomethylation and gene regulation. Nat Immunol 17: 1216–1225. [PubMed: 27500631]
23. Huang da W, Sherman BT, and Lempicki RA 2009 Systematic and integrative analysis of large gene lists using DAVID bioinformatics resources. Nat Protoc 4: 44–57. [PubMed: 19131956]
24. Mootha VK, Lindgren CM, Eriksson KF, Subramanian A, Sihag S, Lehar J, Puigserver P, Carlsson E, Ridderstrale M, Laurila E, Houstis N, Daly MJ, Patterson N, Mesirov JP, Golub TR, Tamayo P, Spiegelman B, Lander ES, Hirschhorn JN, Altshuler D, and Groop LC 2003 PGC-1alpha-responsive genes involved in oxidative phosphorylation are coordinately downregulated in human diabetes. Nat Genet 34: 267–273. [PubMed: 12808457]
25. Buenrostro JD, Giresi PG, Zaba LC, Chang HY, and Greenleaf WJ 2013 Transposition of native chromatin for fast and sensitive epigenomic profiling of open chromatin, DNA-binding proteins and nucleosome position. Nat Methods 10: 1213–1218. [PubMed: 24097267]
26. Guo M, Price MJ, Patterson DG, Barwick BG, Haines RR, Kania AK, Bradley JE, Randall TD, Boss JM, and Scharer CD 2018 EZH2 Represses the B Cell Transcriptional Program and Regulates Antibody-Secreting Cell Metabolism and Antibody Production. J Immunol 200: 1039–1052. [PubMed: 29288200]

27. Langmead B, Trapnell C, Pop M, and Salzberg SL 2009 Ultrafast and memory-efficient alignment of short DNA sequences to the human genome. Genome Biol 10: R25. [PubMed: 19261174]
28. Zhang Y, Liu T, Meyer CA, Eeckhoute J, Johnson DS, Bernstein BE, Nusbaum C, Myers RM, Brown M, Li W, and Liu XS 2008 Model-based analysis of ChIP-Seq (MACS). Genome Biol 9: R137. [PubMed: 18798982]
29. Heinz S, Benner C, Spann N, Bertolino E, Lin YC, Laslo P, Cheng JX, Murre C, Singh H, and Glass CK 2010 Simple combinations of lineage-determining transcription factors prime cis-regulatory elements required for macrophage and B cell identities. Mol Cell 38: 576–589. [PubMed: 20513432]
30. Scharer CD, Blalock EL, Barwick BG, Haines RR, Wei C, Sanz I, and Boss JM 2016 ATAC-seq on biobanked specimens defines a unique chromatin accessibility structure in naive SLE B cells. Sci Rep 6: 27030. [PubMed: 27249108]
31. Zhang K, Wang M, Zhao Y, and Wang W 2019 Taiji: System-level identification of key transcription factors reveals transcriptional waves in mouse embryonic development. Sci Adv 5: eaav3262. [PubMed: 30944857]
32. Epstein MA, Achong BG, Barr YM, Zajac B, Henle G, and Henle W 1966 Morphological and virological investigations on cultured Burkitt tumor lymphoblasts (strain Raji). J Natl Cancer Inst 37: 547–559. [PubMed: 4288580]
33. Dignam JD, Lebovitz RM, and Roeder RG 1983 Accurate transcription initiation by RNA polymerase II in a soluble extract from isolated mammalian nuclei. Nucleic Acids Res 11: 1475–1489. [PubMed: 6828386]
34. Barwick BG, Scharer CD, Martinez RJ, Price MJ, Wein AN, Haines RR, Bally APR, Kohlmeier JE, and Boss JM 2018 B cell activation and plasma cell differentiation are inhibited by de novo DNA methylation. Nat Commun 9: 1900. [PubMed: 29765016]
35. Shi W, Liao Y, Willis SN, Taubenheim N, Inouye M, Tarlinton DM, Smyth GK, Hodgkin PD, Nutt SL, and Corcoran LM 2015 Transcriptional profiling of mouse B cell terminal differentiation defines a signature for antibody-secreting plasma cells. Nat Immunol 16: 663–673. [PubMed: 25894659]
36. Saito T, Chiba S, Ichikawa M, Kunisato A, Asai T, Shimizu K, Yamaguchi T, Yamamoto G, Seo S, Kumano K, Nakagami-Yamaguchi E, Hamada Y, Aizawa S, and Hirai H 2003 Notch2 is preferentially expressed in mature B cells and indispensable for marginal zone B lineage development. Immunity 18: 675–685. [PubMed: 12753744]
37. Alinikula J, Nera KP, Junttila S, and Lassila O 2011 Alternate pathways for Bcl6-mediated regulation of B cell to plasma cell differentiation. Eur J Immunol 41: 2404–2413. [PubMed: 21674482]
38. Winkelmann R, Sandrock L, Porstner M, Roth E, Mathews M, Hobeika E, Reth M, Kahn ML, Schuh W, and Jack HM 2011 B cell homeostasis and plasma cell homing controlled by Kruppel-like factor 2. Proc Natl Acad Sci U S A 108: 710–715. [PubMed: 21187409]
39. Xu Z, Potula HH, Vallurupalli A, Perry D, Baker H, Croker BP, Dozmorov I, and Morel L 2011 Cyclin-dependent kinase inhibitor Cdkn2c regulates B cell homeostasis and function in the NZM2410-derived murine lupus susceptibility locus Sle2c1. J Immunol 186: 6673–6682. [PubMed: 21543644]
40. Dolence JJ, Gwin KA, Shapiro MB, Hsu FC, Shapiro VS, and Medina KL 2015 Cell extrinsic alterations in splenic B cell maturation in Flt3-ligand knockout mice. Immun Inflamm Dis 3: 103–117. [PubMed: 26029370]
41. Quong MW, Martensson A, Langerak AW, Rivera RR, Nemazee D, and Murre C 2004 Receptor editing and marginal zone B cell development are regulated by the helix-loop-helix protein, E2A. J Exp Med 199: 1101–1112. [PubMed: 15078898]
42. Yanai H, Negishi H, and Taniguchi T 2012 The IRF family of transcription factors: Inception, impact and implications in oncogenesis. Oncoimmunology 1: 1376–1386. [PubMed: 23243601]
43. Recaldin T, and Fear DJ 2016 Transcription factors regulating B cell fate in the germinal centre. Clin Exp Immunol 183: 65–75. [PubMed: 26352785]

44. Arguni E, Arima M, Tsuruoka N, Sakamoto A, Hatano M, and Tokuhisa T 2006 JunD/AP-1 and STAT3 are the major enhancer molecules for high Bcl6 expression in germinal center B cells. Int Immunol 18: 1079–1089. [PubMed: 16702165]
45. Wong KK, Khatri I, Shaha S, Spaner DE, and Gorczynski RM 2010 The role of CD200 in immunity to B cell lymphoma. J Leukoc Biol 88: 361–372. [PubMed: 20442224]
46. Ettinger R, Kuchen S, and Lipsky PE 2008 The role of IL-21 in regulating B-cell function in health and disease. Immunol Rev 223: 60–86. [PubMed: 18613830]
47. Xie H, Ye M, Feng R, and Graf T 2004 Stepwise reprogramming of B cells into macrophages. Cell 117: 663–676. [PubMed: 15163413]
48. Santos A, Tsafou K, Stolte C, Pletscher-Frankild S, O'Donoghue SI, and Jensen LJ 2015 Comprehensive comparison of large-scale tissue expression datasets. PeerJ 3: e1054. [PubMed: 26157623]
49. Wu C, Macleod I, and Su AI 2013 BioGPS and MyGene.info: organizing online, gene-centric information. Nucleic Acids Res 41: D561–565. [PubMed: 23175613]
50. Eyquem S, Chemin K, Fasseu M, Chopin M, Sigaux F, Cumano A, and Bories JC 2004 The development of early and mature B cells is impaired in mice deficient for the Ets-1 transcription factor. Eur J Immunol 34: 3187–3196. [PubMed: 15384043]
51. Willis SN, Tellier J, Liao Y, Trezise S, Light A, O'Donnell K, Garrett-Sinha LA, Shi W, Tarlinton DM, and Nutt SL 2017 Environmental sensing by mature B cells is controlled by the transcription factors PU.1 and SpiB. Nat Commun 8: 1426. [PubMed: 29127283]
52. Zhang XK, Moussa O, LaRue A, Bradshaw S, Molano I, Spyropoulos DD, Gilkeson GS, and Watson DK 2008 The transcription factor Fli-1 modulates marginal zone and follicular B cell development in mice. J Immunol 181: 1644–1654. [PubMed: 18641300]
53. Wikstrom I, Forssell J, Goncalves M, Colucci F, and Holmberg D 2006 E2–2 regulates the expansion of pro-B cells and follicular versus marginal zone decisions. J Immunol 177: 6723–6729. [PubMed: 17082585]
54. Almaden JV, Liu YC, Yang E, Otero DC, Birnbaum H, Davis-Turak J, Asagiri M, David M, Goldrath AW, and Hoffmann A 2016 B-cell survival and development controlled by the coordination of NF-kappaB family members RelB and cRel. Blood 127: 1276–1286. [PubMed: 26773039]
55. De Silva NS, Silva K, Anderson MM, Bhagat G, and Klein U 2016 Impairment of Mature B Cell Maintenance upon Combined Deletion of the Alternative NF-kappaB Transcription Factors RELB and NF-kappaB2 in B Cells. J Immunol 196: 2591–2601. [PubMed: 26851215]
56. Emslie D, D'Costa K, Hasbold J, Metcalf D, Takatsu K, Hodgkin PO, and Corcoran LM 2008 Oct2 enhances antibody-secreting cell differentiation through regulation of IL-5 receptor alpha chain expression on activated B cells. J Exp Med 205: 409–421. [PubMed: 18250192]
57. Cusan M, Cai SF, Mohammad HP, Krivtsov A, Chramiec A, Loizou E, Witkin MD, Smitheman KN, Tenen DG, Ye M, Will B, Steidl U, Kruger RG, Levine RL, Rienhoff HY Jr., Koche RP, and Armstrong SA 2018 LSD1 inhibition exerts its antileukemic effect by recommissioning PU.1- and C/EBPalpha-dependent enhancers in AML. Blood 131: 1730–1742. [PubMed: 29453291]
58. Choi J, Jang H, Kim H, Kim ST, Cho EJ, and Youn HD 2010 Histone demethylase LSD1 is required to induce skeletal muscle differentiation by regulating myogenic factors. Biochem Biophys Res Commun 401: 327–332. [PubMed: 20833138]
59. Li Y, Deng C, Hu X, Patel B, Fu X, Qiu Y, Brand M, Zhao K, and Huang S 2012 Dynamic interaction between TAL1 oncoprotein and LSD1 regulates TAL1 function in hematopoiesis and leukemogenesis. Oncogene 31: 5007–5018. [PubMed: 22310283]
60. Kim D, Nam HJ, Lee W, Yim HY, Ahn JY, Park SW, Shin HR, Yu R, Won KJ, Bae JS, Kim KI, and Baek SH 2018 PKCalpha-LSD1-NF-kappaB-Signaling Cascade Is Crucial for Epigenetic Control of the Inflammatory Response. Mol Cell 69: 398–411 e396. [PubMed: 29395062]
61. Vilagos B, Hoffmann M, Souabni A, Sun Q, Werner B, Medvedovic J, Bilic I, Minnich M, Axelsson E, Jaritz M, and Busslinger M 2012 Essential role of EBF1 in the generation and function of distinct mature B cell types. J Exp Med 209: 775–792. [PubMed: 22473956]
62. Capellini TD, Di Giacomo G, Salsi V, Brendolan A, Ferretti E, Srivastava D, Zappavigna V, and Selleri L 2006 Pbx1/Pbx2 requirement for distal limb patterning is mediated by the hierarchical

control of Hox gene spatial distribution and Shh expression. Development 133: 2263–2273. [PubMed: 16672333]

63. Vlachakis N, Choe SK, and Sagerstrom CG 2001 Meis3 synergizes with Pbx4 and Hoxb1b in promoting hindbrain fates in the zebrafish. Development 128: 1299–1312. [PubMed: 11262231]
64. Subramanian A, Tamayo P, Mootha VK, Mukherjee S, Ebert BL, Gillette MA, Paulovich A, Pomeroy SL, Golub TR, Lander ES, and Mesirov JP 2005 Gene set enrichment analysis: a knowledge-based approach for interpreting genome-wide expression profiles. Proc Natl Acad Sci U S A 102: 15545–15550. [PubMed: 16199517]
65. Grinberg-Bleyer Y, Caron R, Seeley JJ, De Silva NS, Schindler CW, Hayden MS, Klein U, and Ghosh S 2018 The Alternative NF-kappaB Pathway in Regulatory T Cell Homeostasis and Suppressive Function. J Immunol 200: 2362–2371. [PubMed: 29459403]
66. Vasanthakumar A, Liao Y, Teh P, Pascutti MF, Oja AE, Garnham AL, Gloury R, Tempany JC, Sidwell T, Cuadrado E, Tuijnenburg P, Kuijpers TW, Lalaoui N, Mielke LA, Bryant VL, Hodgkin PD, Silke J, Smyth GK, Nolte MA, Shi W, and Kallies A 2017 The TNF Receptor Superfamily-NF-kappaB Axis Is Critical to Maintain Effector Regulatory T Cells in Lymphoid and Non-lymphoid Tissues. Cell Rep 20: 2906–2920. [PubMed: 28889989]
67. Zhao M, Joy J, Zhou W, De S, Wood WH 3rd, Becker KG, Ji H, and Sen R 2018 Transcriptional outcomes and kinetic patterning of gene expression in response to NF-kappaB activation. PLoS Biol 16: e2006347. [PubMed: 30199532]
68. Doumont G, Martoriati A, and Marine JC 2005 PTPRV is a key mediator of p53-induced cell cycle exit. Cell Cycle 4: 1703–1705. [PubMed: 16258284]
69. Latonen L, Jarvinen PM, and Laiho M 2008 Cytoskeleton-interacting LIM-domain protein CRP1 suppresses cell proliferation and protects from stress-induced cell death. Exp Cell Res 314: 738–747. [PubMed: 18177859]
70. Bradfute SB, Graubert TA, and Goodell MA 2005 Roles of Sca-1 in hematopoietic stem/progenitor cell function. Exp Hematol 33: 836–843. [PubMed: 15963860]
71. Funakoshi S, Shimizu T, Numata O, Ato M, Melchers F, and Ohnishi K 2015 BILL-cadherin/cadherin-17 contributes to the survival of memory B cells. PLoS One 10: e0117566. [PubMed: 25612318]
72. Brown RT, Ades IZ, and Nordan RP 1995 An acute phase response factor/NF-kappa B site downstream of the junB gene that mediates responsiveness to interleukin-6 in a murine plasmacytoma. J Biol Chem 270: 31129–31135. [PubMed: 8537375]
73. Marques L, Brucet M, Lloberas J, and Celada A 2004 STAT1 regulates lipopolysaccharide- and TNF-alpha-dependent expression of transporter associated with antigen processing 1 and low molecular mass polypeptide 2 genes in macrophages by distinct mechanisms. J Immunol 173: 1103–1110. [PubMed: 15240699]
74. Hopken UE, Foss HD, Meyer D, Hinz M, Leder K, Stein H, and Lipp M 2002 Up-regulation of the chemokine receptor CCR7 in classical but not in lymphocyte-predominant Hodgkin disease correlates with distinct dissemination of neoplastic cells in lymphoid organs. Blood 99: 1109–1116. [PubMed: 11830455]
75. Fairfax KA, Corcoran LM, Pridans C, Huntington ND, Kallies A, Nutt SL, and Tarlinton DM 2007 Different kinetics of blimp-1 induction in B cell subsets revealed by reporter gene. J Immunol 178: 4104–4111. [PubMed: 17371965]
76. Almeida LO, Abrahao AC, Rosselli-Murai LK, Giudice FS, Zagni C, Leopoldino AM, Squarize CH, and Castilho RM 2014 NFkappaB mediates cisplatin resistance through histone modifications in head and neck squamous cell carcinoma (HNSCC). FEBS Open Bio 4: 96–104.
77. Nakshatri H, Appaiah HN, Anjanappa M, Gilley D, Tanaka H, Badve S, Crooks PA, Mathews W, Sweeney C, and Bhat-Nakshatri P 2015 NF-kappaB-dependent and -independent epigenetic modulation using the novel anti-cancer agent DMAPT. Cell Death Dis 6: e1608. [PubMed: 25611383]
78. van Essen D, Zhu Y, and Saccani S 2010 A feed-forward circuit controlling inducible NF-kappaB target gene activation by promoter histone demethylation. Mol Cell 39: 750–760. [PubMed: 20832726]

79. Wietek C, Cleaver CS, Ludbrook V, Wilde J, White J, Bell DJ, Lee M, Dickson M, Ray KP, and O'Neill LA 2006 IkappaB kinase epsilon interacts with p52 and promotes transactivation via p65. J Biol Chem 281: 34973–34981. [PubMed: 17003035]

80. Dong J, Jimi E, Zhong H, Hayden MS, and Ghosh S 2008 Repression of gene expression by unphosphorylated NF-kappaB p65 through epigenetic mechanisms. Genes Dev 22: 1159–1173. [PubMed: 18408078]

81. Rocha S, Martin AM, Meek DW, and Perkins ND 2003 p53 represses cyclin D1 transcription through down regulation of Bcl-3 and inducing increased association of the p52 NF-kappaB subunit with histone deacetylase 1. Mol Cell Biol 23: 4713–4727. [PubMed: 12808109]

82. Kratchmarov R, Viragova S, Kim MJ, Rothman NJ, Liu K, Reizis B, and Reiner SL 2018 Metabolic control of cell fate bifurcations in a hematopoietic progenitor population. Immunol Cell Biol 96: 863–871. [PubMed: 29570858]

83. Lin WH, Adams WC, Nish SA, Chen YH, Yen B, Rothman NJ, Kratchmarov R, Okada T, Klein U, and Reiner SL 2015 Asymmetric PI3K Signaling Driving Developmental and Regenerative Cell Fate Bifurcation. Cell Rep 13: 2203–2218. [PubMed: 26628372]

84. Wu H, Deng Y, Feng Y, Long D, Ma K, Wang X, Zhao M, Lu L, and Lu Q 2018 Epigenetic regulation in B-cell maturation and its dysregulation in autoimmunity. Cell Mol Immunol 15: 676–684. [PubMed: 29375128]

85. Li R, Cauchy P, Ramamoorthy S, Boller S, Chavez L, and Grosschedl R 2018 Dynamic EBF1 occupancy directs sequential epigenetic and transcriptional events in B-cell programming. Genes Dev 32: 96–111. [PubMed: 29440261]

86. Song Y, Wu F, and Wu J 2016 Targeting histone methylation for cancer therapy: enzymes, inhibitors, biological activity and perspectives. J Hematol Oncol 9: 49. [PubMed: 27316347]

87. Szyf M 2010 Epigenetic therapeutics in autoimmune disease. Clin Rev Allergy Immunol 39: 62–77. [PubMed: 19644776]

88. Joshi M, Sheikh H, Abbi K, Long S, Sharma K, Tulchinsky M, and Epner E 2012 Marginal zone lymphoma: old, new, targeted, and epigenetic therapies. Ther Adv Hematol 3: 275–290. [PubMed: 23616915]

Key Points

1. LSD1 is necessary for marginal zone B cell development
2. LSD1 repressors the follicular B cell program
3. With non-canonical NF-κB, LSD1 regulates marginal zone B cell development

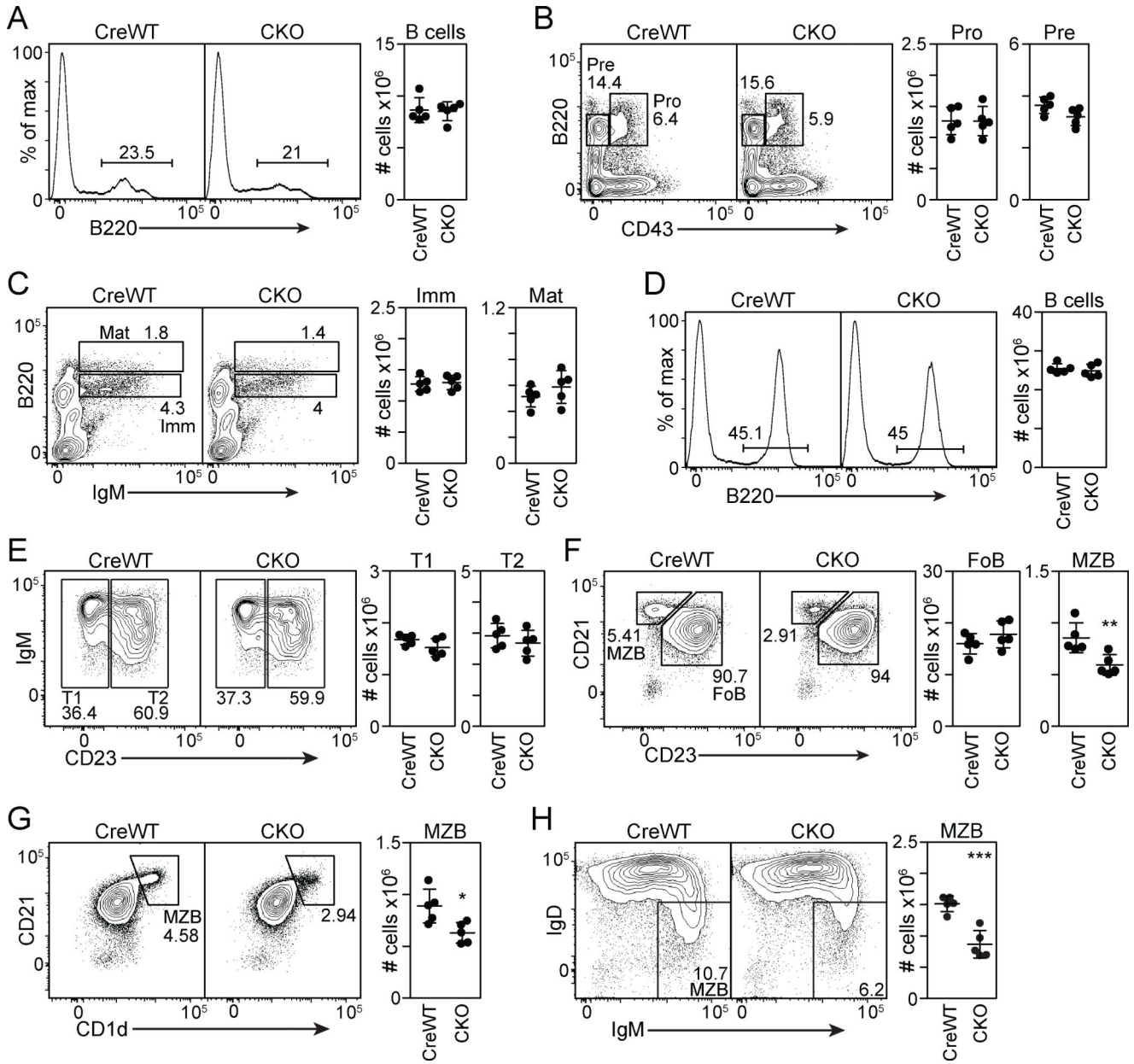

Figure 1 –. B cell conditional LSD1 deletion results in fewer marginal zone B cells

(A-C) Flow cytometry analysis of the expression of developing B cell markers in the bone marrow of unstimulated naïve CreWT and CKO mice. Analysis of CreWT and CKO total cell numbers of the following B cell populations are shown: **(A)** $B220^+$ B cells; **(B)** $IgM^-B220^+CD43^+$ pro-B cells and $IgM^-B220^+CD43^-$ pre-B cells; **(C)** IgM^+B220^{mid} immature B cells and IgM^+B220^{hi} mature B cells. **(D-H)** Flow cytometry analysis of the expression of developing B cell markers in the spleen of unstimulated CreWT and CKO mice. Analysis of CreWT and CKO total cell numbers of the following B cell populations are shown: **(D)** $B220^+$ B cells; **(E)** $B220^+CD93^+CD23^-$ T1 and $B220^+CD93^+CD23^+$ T2 B cells; **(F)** $B220^+CD93^-CD21^{hi}CD23^-$ MZB and $B220^+CD93^-CD21^{mid}CD23^+$ FoB; **(G)** $B220^+CD93^-CD21^{hi}CD1d^+$ MZB; **(H)** $B220^+CD93^-IgM^+IgD^-$ MZB. All data are representative of at

least two independent experiments using three to five mice per group. Error bars represent mean ± SD. Significance was determined by Student's two-tailed *t*-test. **P*<0.05, ***P*<0.01, ****P*<0.001.

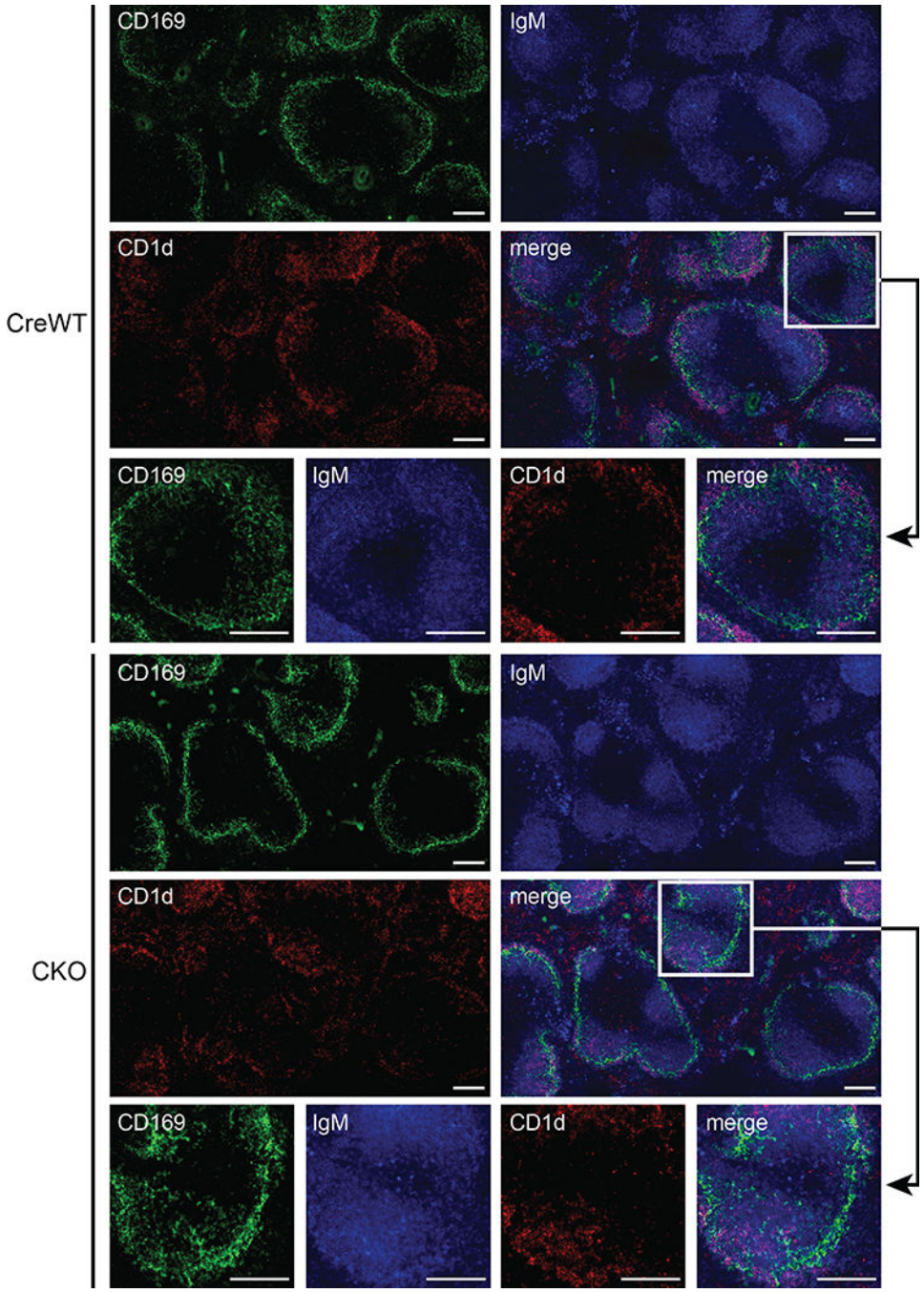

Figure 2 –. B cell conditional LSD1 deletion mouse spleens display normal marginal zone architecture

Immunofluorescence staining for CD169 (green), IgM (blue), and CD1d (red) in the spleens of CreWT and CKO mice. Images are at 10X magnification. Scale bars, 400 μm.

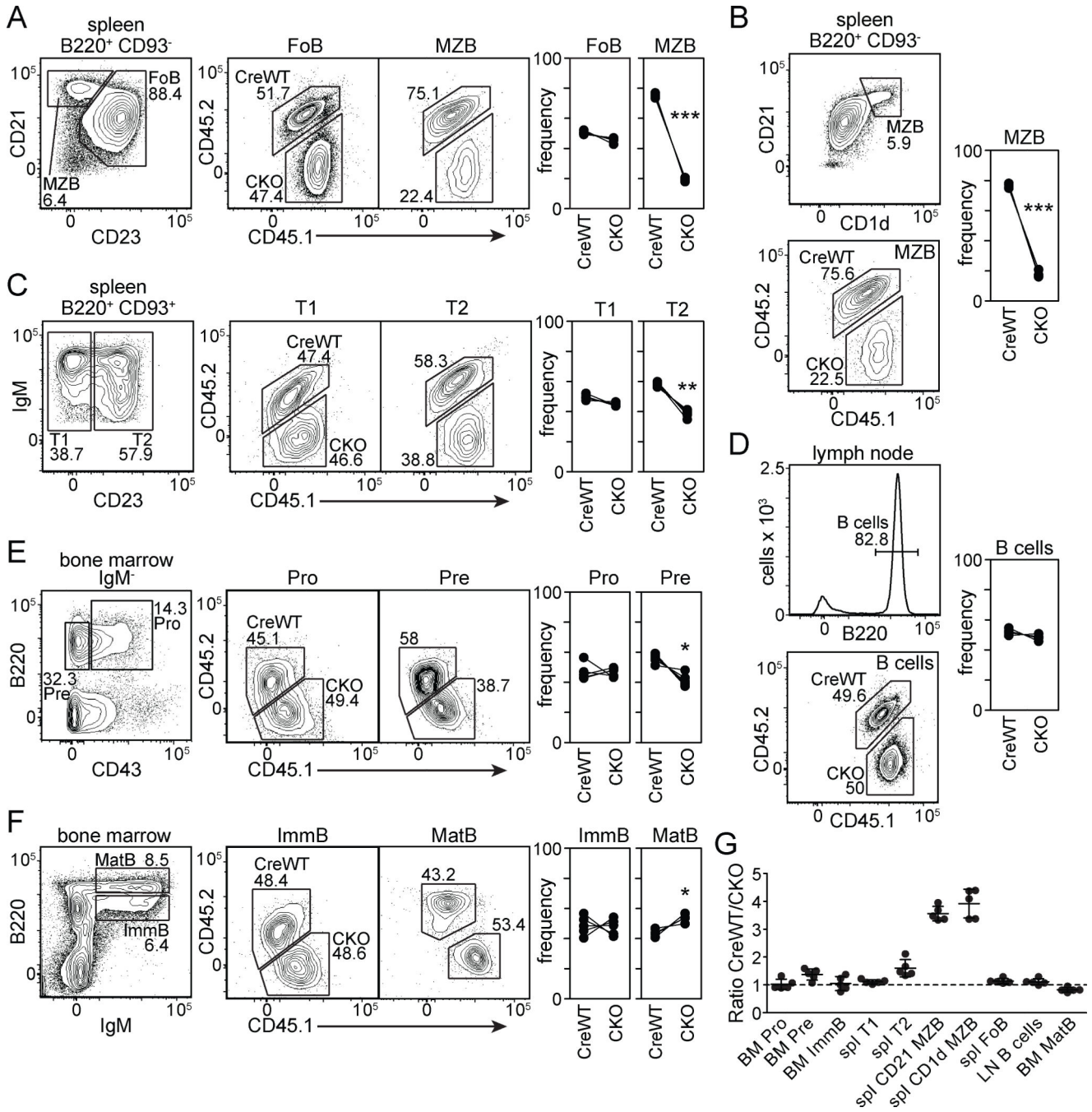

Figure 3 –. Reduction of LSD1-deficient marginal zone B cells is cell-intrinsic

(A-F) Flow cytometry analysis of the expression of developing B cell markers in the spleen and bone marrow of unstimulated mixed bone marrow chimera mice reconstituted in a 50:50 ratio of CKO and CreWT bone marrow. Analysis of CreWT and CKO frequencies of the following B cell populations are shown: **(A)** splenic $B220^{+}CD93^{-}CD21^{mid}CD23^{+}$ FoB and $B220^{+}CD93^{-}CD21^{+}CD23^{-}$ MZB; **(B)** splenic $B220^{+}CD93^{-}CD21^{hi}CD1d^{+}$ MZB; **(C)** splenic $B220^{+}CD93^{+}CD23^{-}$ T1 B cells and $B220^{+}CD93^{+}CD23^{+}$ T2 B cells; **(D)** lymph node $B220^{+}$ B cells; **(E)** bone marrow $IgM^{-}B220^{+}CD43^{+}$ pro-B cells and $IgM^{-}B220^{+}CD43^{-}$

pre-B cells; **(F)** bone marrow IgM^+B220^{mid} immature B cells and IgM^+B220^{hi} mature B cells. **(G)** Ratios of CreWT/CKO frequencies of B cell populations per mouse. All data are representative of two independent experiments using five mice per group. Error bars represent mean ± SD. Significance was determined by Student's paired two-tailed *t*-test. $*P<0.05$, $**P<0.01$, $***P<0.001$.

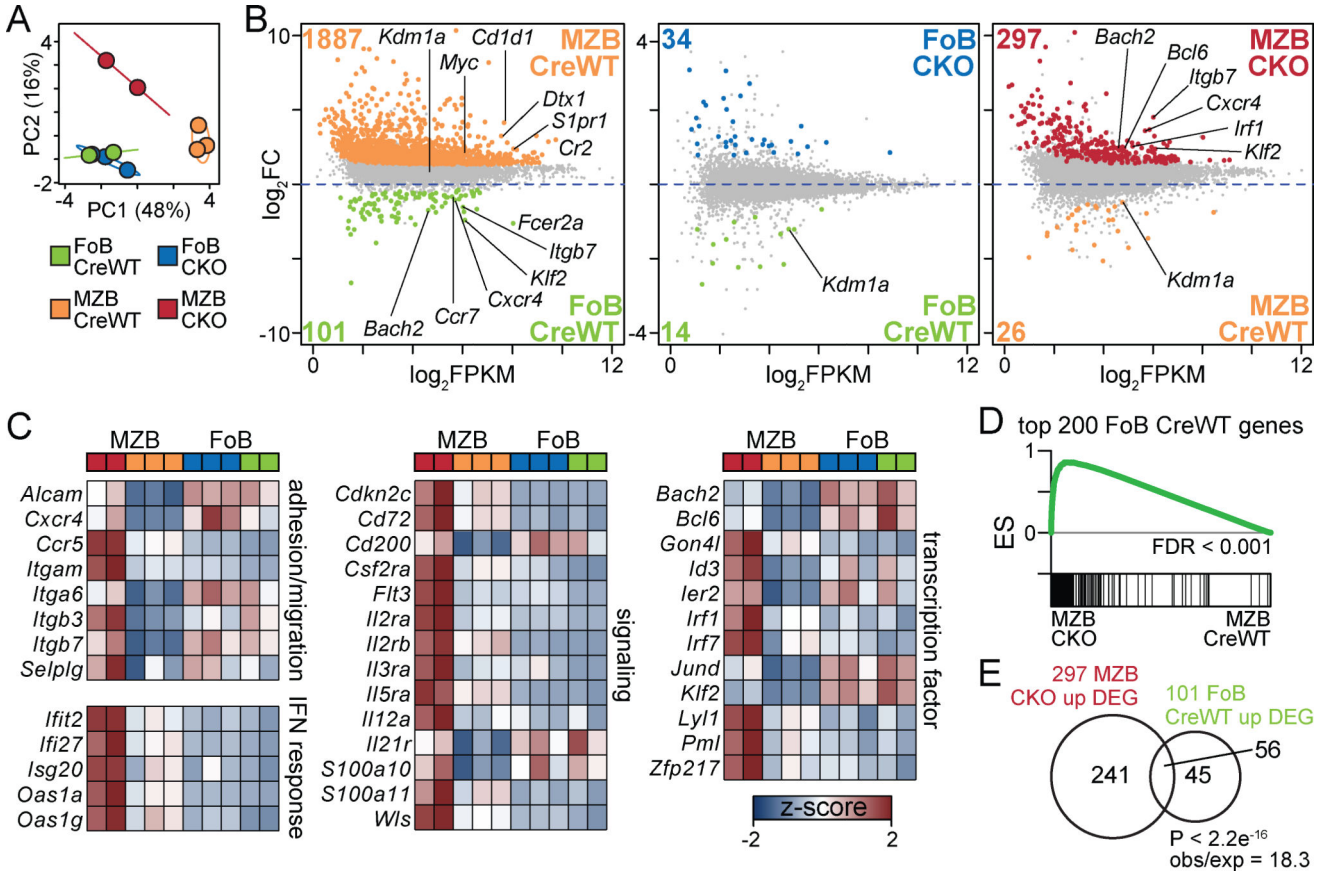

Figure 4 –. LSD1 functions as a transcriptional repressor in marginal zone B cells

(A) Top two principal components from PCA of z-score normalized mRNA/cell expression of all 9,690 detected genes in all samples. **(B)** Scatterplots of log_2FC vs. log_2FPKM data from differential expression analysis comparing MZB CreWT (orange) and FoB CreWT (green), FoB CKO (blue) vs. FoB CreWT (green), and MZB CKO (red) vs. MZB CreWT (orange). **(C)** Heatmaps of z-score normalized mRNA/cell expression of genes in KEGG pathways or functional catagories. **(D)** GSEA plot displaying the enrichment of the top 200 most significant genes upregulated in MZB CreWT relative to FoB CreWT within the MZB CKO vs. MZB CreWT ranked gene list. **(E)** Overlapping DEG between the indicated comparison. Significance was determined by Fisher's exact test. Observed/expected (obs/exp) refers to the ratio of observed DEG overlap over expected overlap according to a permutation test.

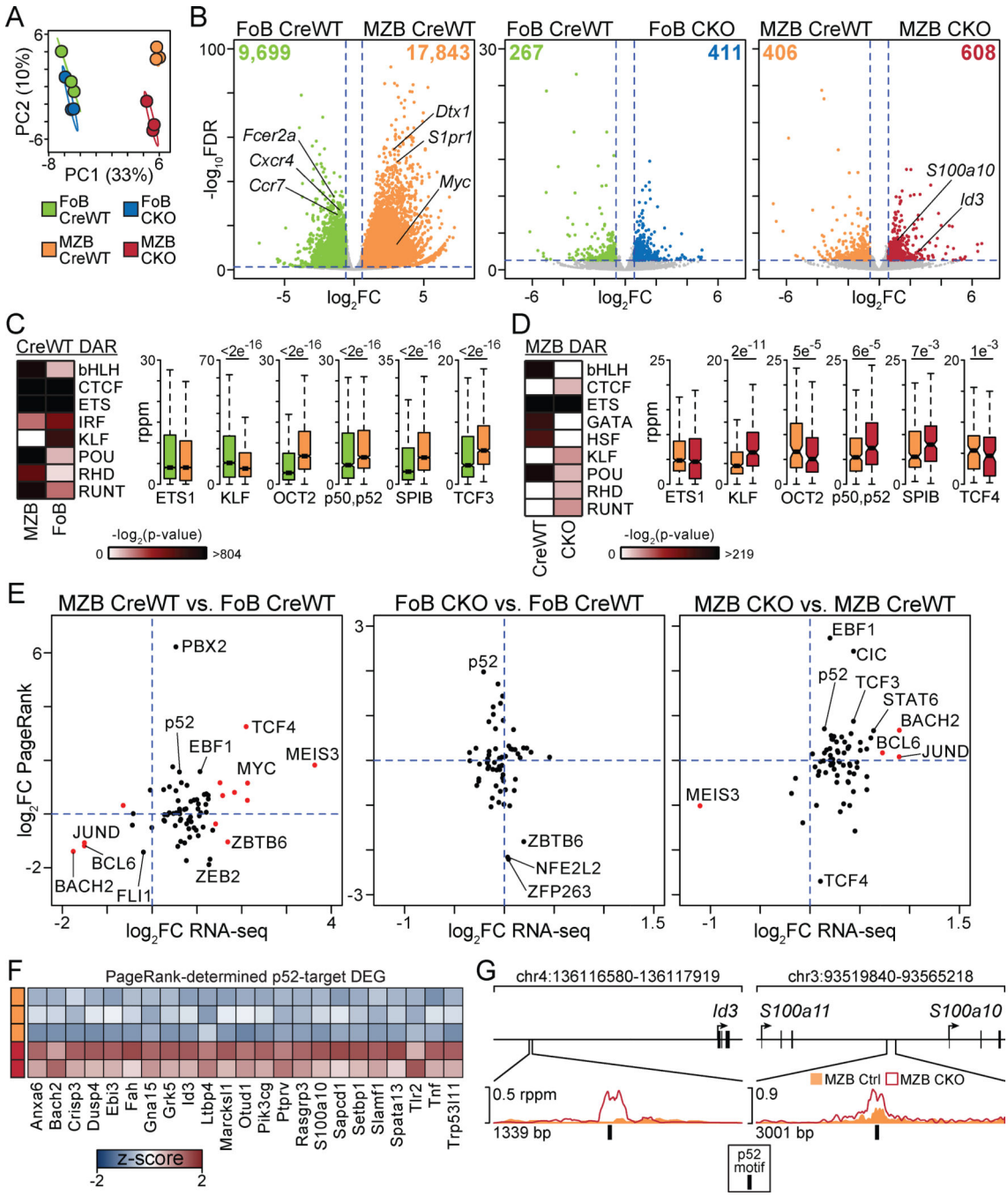

Figure 5 –. LSD1 regulates chromatin accessibility at NF-κB motifs

(A) Top two principal components from PCA of z-score normalized rppm accessibility data of all 94,161 detected peaks in all samples. **(B)** Volcano plots of -$\log_{10}$FDR vs. $\log_2$FC from differential accessibility analysis on three different sample group comparisons. **(C,D)** Heatmap displaying –$\log_2$(*P* values) of top significantly enriched transcription factor family motifs for the indicated DAR groups from B. Boxplots depict rppm enrichment of chromatin accessibility for the indicated sample group at specific transcription factor motifs. Significance was determined by Student's two-tailed *t*-test. **(E)** Scatterplots of $\log_2$FC data

from PageRank analysis vs. $\log_2$FC data from RNA-seq analysis on three different sample group comparisons. Points correspond to transcription factors with a PageRank score >0.003 (top 10%) in at least one of the compared sample groups. A red point indicates a DEG in the given comparison. **(F)** Heatmap of z-score normalized mRNA/cell expression of p52-target genes predicted by PageRank analysis. **(G)** Gene track examples of rppm chromatin accessibility data for DAR that increase in accessibility in MZB CKO that map to a p52 motif and a p52-target DEG predicted by PageRank analysis.

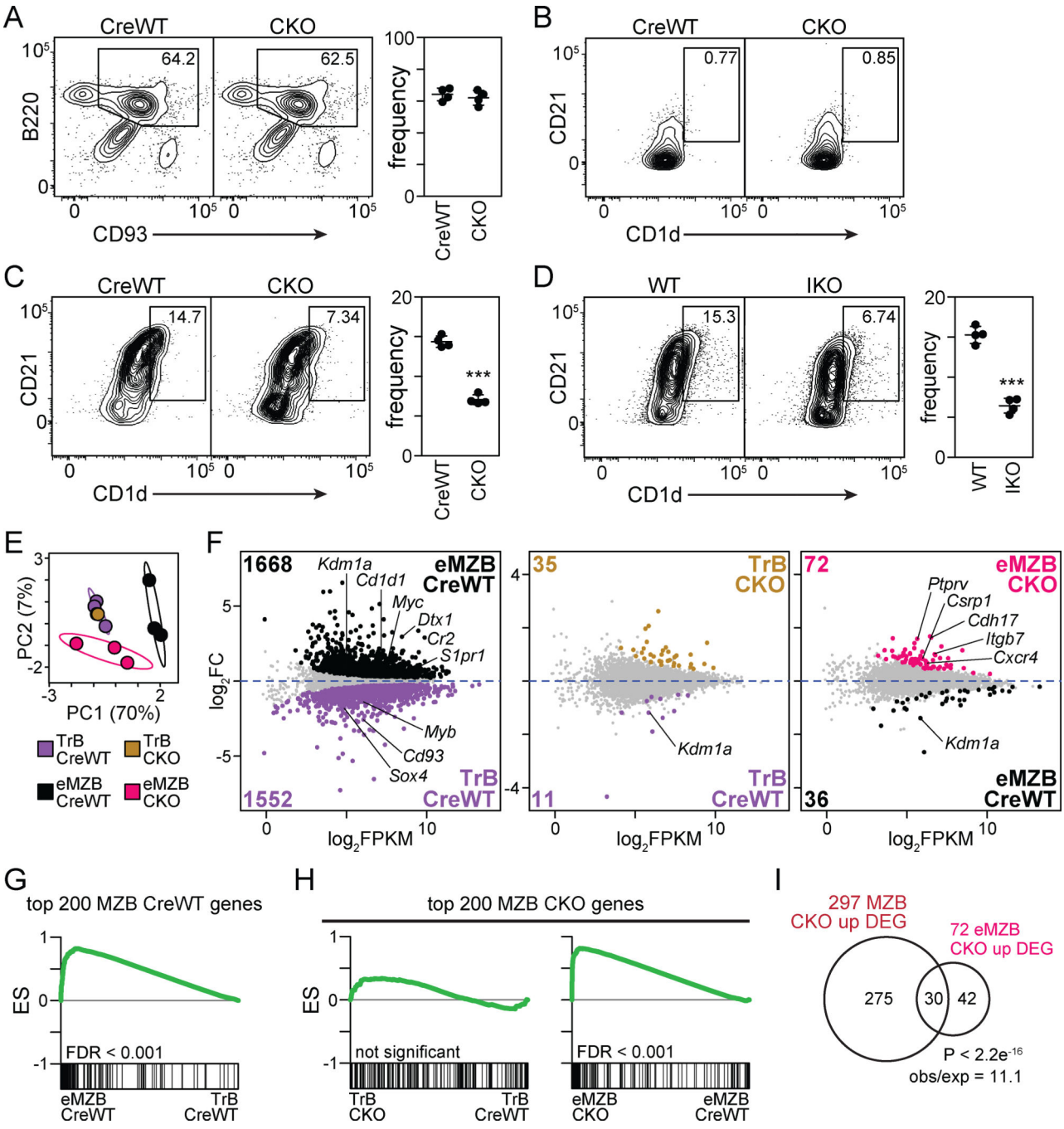

Figure 6 –. LSD1 regulates *ex vivo* marginal zone B cell development

(A) Flow cytometry analysis of B220 and CD93 expression on PE^{+} enrichments of CD93-PE-stained spleens from CreWT and CKO mice. **(B)** CD21 and CD1d expression on gated populations from part A. **(C)** CD21 and CD1d expression on B220^{+} CKO or CreWT cells after three days of being cultured with OP9-DL1 cells in the presence of BAFF. **(D)** CD21 and CD1d expression on B220^{+} IKO or WT cells after three days of being cultured with OP9-DL1 cells in the presence of BAFF. Cells were cultured five days after a five day tamoxifen treatment regimen. **(E)** Top two principal components from PCA of z-score

normalized mRNA/cell expression of all 9,843 detected genes in all samples. **(F)** Scatterplots of log_2FC vs. log_2FPKM data from differential expression analysis for the indicated sample group comparisons. **(G)** GSEA plot displaying the enrichment of the top 200 most significant genes upregulated in MZB CreWT relative to FoB CreWT within the eMZB CreWT vs. TrB CreWT ranked gene list. **(H)** GSEA plots displaying the enrichment of the top 200 most significant genes upregulated in MZB CKO relative to MZB CreWT within two ranked gene lists: TrB CKO vs. TrB CreWT and eMZB CKO vs. eMZB CreWT. **(I)** Overlapping DEG between the indicated comparison. Significance was determined by Student's two-tailed *t*-test (A,C,D) and Fisher's exact test (I). Observed/expected (obs/exp) refers to the ratio of observed DEG overlap over expected overlap according to a permutation test.

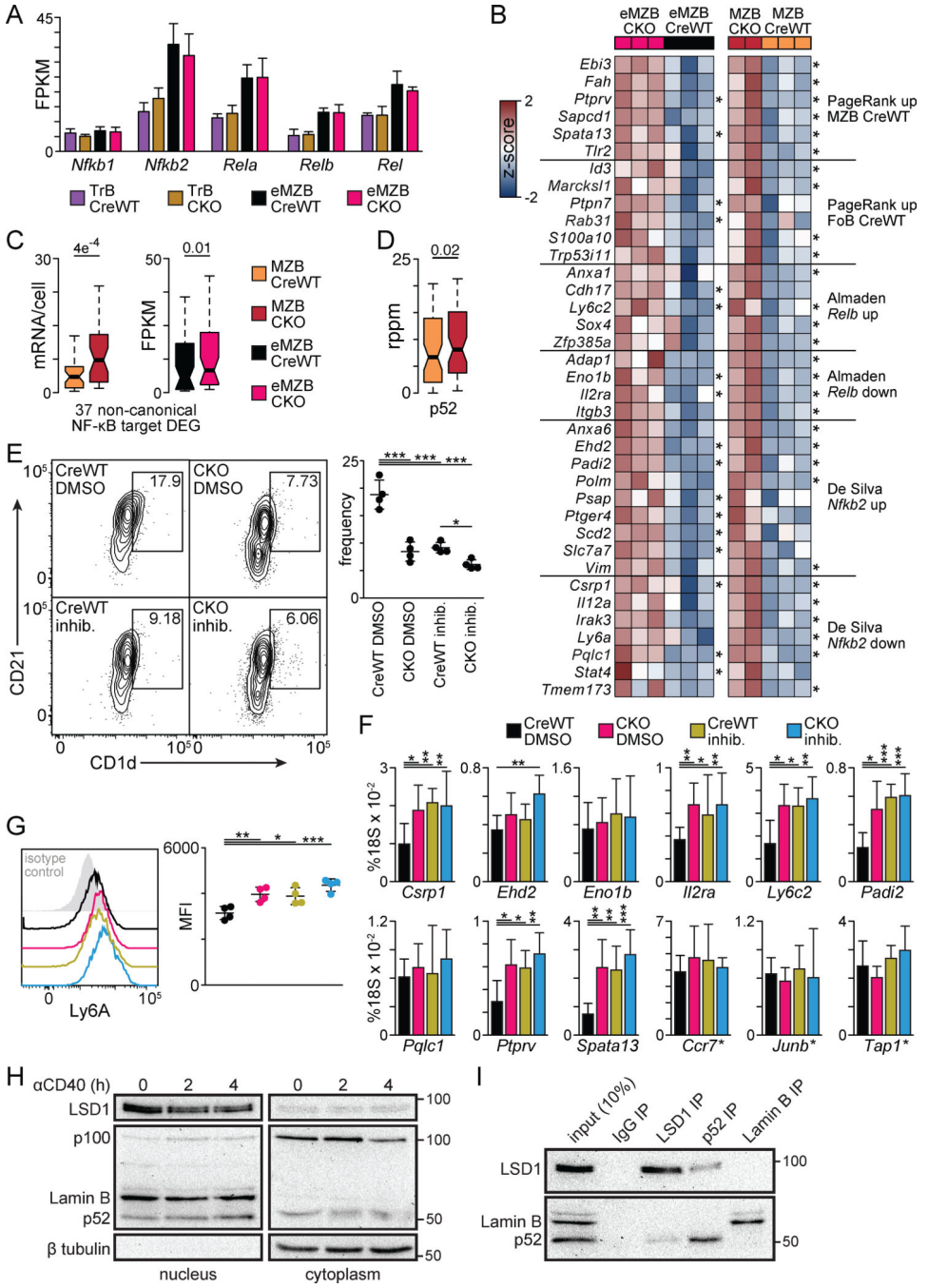

Figure 7 –. LSD1 and NF-κB cooperate to regulate marginal zone B cell development

(A) FPKM expression of NF-κB transcription factors. **(B)** Heatmaps of z-score normalized mRNA/cell and FPKM expression of 37 genes that are DEG in both sample groups or are a DEG in one group and trending up in the other. DEG are denoted by *. **(C)** Box plots of mRNA/cell or FPKM expression of the 37 genes displayed in B. **(D)** Box plot of rppm enrichment of chromatin accessibility at p52 motifs that map to the 37 genes displayed in B. **(E)** Flow cytometry analysis of CD21 and CD1d expression on B220^{+} CKO or CreWT cells after three days of being cultured with OP9-DL1 cells in the presence of BAFF. Cells were

treated with either the NF-κB inhibitor IKK-16 (inhib.) or DMSO. **(F)** RT-qPCR expression data relative to 18S expression of select genes. Canonical NF-κB target genes are denoted by *. **(G)** Flow cytometry analysis of Ly6A/ for the four populations of cells gated in part E. **(H)** Western blot of Raji cell nuclear and cytoplasmic lysates collected following zero, two, and four hours of αCD40 Ab treatment. **(I)** Co-immunoprecipitations from Raji cell nuclear extracts at four hours following αCD40 Ab treatment. All flow cytometry data are representative of two independent experiments using four to five mice per group. Error bars represent mean ± SD. Significance was determined by Student's paired two-tailed *t*-test. $*P<0.05$, $**P<0.01$, $***P<0.001$.